

# **Divergent Biophysical Responses of Western United States Forests to Wildfire Driven by Eco-climatic Gradients**

Surendra Shrestha<sup>1\*</sup>, Christopher A. Williams<sup>1</sup>, Brendan M. Rogers<sup>2</sup>, John Rogan<sup>1</sup>, and Dominik Kulakowski<sup>1</sup>

<sup>1</sup>Graduate School of Geography, Clark University, Worcester, MA 01610

<sup>2</sup>Woods Hole Research Center, Falmouth, MA 02540

\*Corresponding Author:

Surendra Shrestha

Graduate School of Geography, Clark University

Worcester, MA 01610

Email: [Surshrestha@clarku.edu](mailto:Surshrestha@clarku.edu); [sbs.stha111@gmail.com](mailto:sbs.stha111@gmail.com)

Phone: +1- (774) 253-0917

1    **Abstract**

2    Understanding vegetation recovery after fire is critical for predicting vegetation-mediated  
3    ecological dynamics in future climates. However, information characterizing vegetation recovery  
4    patterns after fire and their determinants are limited over large geographical extents. This study  
5    uses Moderate Resolution Imaging Spectroradiometer (MODIS) leaf area index (LAI) and albedo  
6    to characterize patterns of post-fire biophysical dynamics across the western United States (US)  
7    and further examines the influence of topo-climatic variables on the recovery of LAI and albedo  
8    at two different time horizons, 10 and 20 years post-fire, using a random forest model. Recovery  
9    patterns were derived for all wildfires that occurred between 1986 and 2017 across seven forest  
10   types and 21 level III ecoregions of the western US. We found differences in characteristic  
11   trajectories of post-fire vegetation recovery across forest types and ecoclimatic settings. LAI in  
12   some forest types recovered only 60% - 70% by 25 years after fire while it recovered 120% to  
13   150% of the pre-fire levels in other forest types, with higher absolute post-fire changes in forest  
14   types and ecoregions that had a higher initial pre-fire LAI. Our random forest results showed very  
15   little influence of fire severity on the recovery of both summer LAI and albedo at both post-fire  
16   time horizons. Post-fire vegetation recovery was most strongly controlled by elevation, with faster  
17   rates of recovery in lower elevations. Similarly, annual precipitation and average summer  
18   temperature had significant impacts on the post-fire recovery of vegetation. Full recovery was  
19   seldom observed when annual precipitation was less than 500 mm and average summer  
20   temperature was above the optimal range i.e., 15-20°C. Climate influences, particularly annual  
21   precipitation, was a major driver of post-fire summer albedo change through its impact on  
22   ecological succession. This study provides quantitative measures of primary controls that could be  
23   used to improve the modelling of ecosystem dynamics post-fire.

24

25   Keywords: wildfire; MODIS; post-fire recovery; biogeophysical; remote sensing; succession

26 **1. Introduction**

27 Wildfires have burned millions of hectares of forests in the western United States (Littell et al.,  
28 2009; White et al., 2017) and have increased in both frequency and severity in recent decades. This  
29 trend has been attributed to temperature increases, more frequent droughts, below average winter  
30 precipitation and earlier spring snowmelt (Dale et al., 2001; Westerling et al., 2006; Rogers et al.,  
31 2011; Ghimire et al., 2012; Dennison et al., 2014; Littell et al., 2015; Abatzoglou & Williams,  
32 2016; Williams & Abatzoglou, 2016; Williams et al., 2021), making ecosystem resilience and  
33 vegetation recovery post-fire a primary concern to researchers and land managers (Allen &  
34 Breshears, 2015). Existing studies report that large wildfires in western U.S. forests have increased  
35 four-fold since 1970-1986, with total burn area increasing by six and a half times (Westerling et  
36 al., 2006). Expanded burning can profoundly alter a wide range of ecosystem characteristics such  
37 as stand structure, species composition, leaf area, canopy ecophysiology, and microclimate (Liu et  
38 al., 2005). The most immediate biophysical effect of wildfire on the land surface is the decrease in  
39 live vegetation and the deposition of black carbon on the soil surface (De Sales et al., 2018). The  
40 alteration in surface roughness directly influences the interaction between the land and the  
41 atmosphere by, typically, reducing the turbulent mixing and net radiation (Chambers et al., 2005).  
42 Moreover, the deposition of the black carbon on the surface changes net radiation through its  
43 impact on surface albedo, which alters the partitioning of energy into latent heat and sensible heat  
44 (Jin & Roy, 2005). Fires have the potential to modify local to regional climate through these long-  
45 lived changes in land surface dynamics and other substantial forcing impacts such as greenhouse  
46 gas fluxes and aerosols (Bonan et al., 1995). In this study, we use contemporary spaceborne  
47 observing systems to quantify the magnitude and timing of ecosystem responses to severe wildfires  
48 as a crucial step in assessing their associated ecological, hydrological, and biogeophysical impacts.

49 In addition to quantification, it is equally important to document the factors that determine  
50 variability in post-fire recovery in order to develop a predictive understanding of ecosystem  
51 dynamics in response to wildfire, especially considering present and expected future increases in  
52 the frequency of large, severe wildfires (Scholze et al., 2006; IPCC, 2007; Seastedt et al., 2008;  
53 Urza et al., 2017; Hankin et al., 2019). Vegetation recovery is likely to vary considerably across  
54 the landscape, even when initial estimates of fire severity are similar (Keeley et al., 2008; Frazier  
55 et al., 2018). Some forest ecosystems have shown to recover fully after large severe disturbances  
56 (Rodrigo et al., 2004; Knox & Clarke, 2012), while others have recovered little towards pre-fire  
57 levels (Barton, 2002; Rodrigo et al., 2004; Lippok et al., 2013). Variability in recovery rates has  
58 been shown to depend on the interactive effects of numerous biotic and abiotic factors related to  
59 nature of fire, life history traits of species, and environmental conditions following fire (Chambers  
60 et al., 2016; Johnstone et al., 2016; Stevens-Rumann et al., 2018). For example, post-fire recovery  
61 of dry mixed conifer forests in the western U.S. is strongly affected by fire severity (Chappell  
62 1996; Meng et al., 2015; Kemp et al., 2016; Harvey et al., 2016; Meng et al., 2018; Vanderhoof et  
63 al., 2020) and pre-fire condition (Martin-Alcon & Coll, 2016; Zhao et al., 2016). Other factors that  
64 can be important to vegetation recovery after fire include vegetation type (Epting, 2005; Yang et  
65 al., 2017); site topography including slope, aspect, and elevation (Wittenberg et al., 2007; Meng  
66 et al., 2015; Liu et al., 2016; Chambers et al., 2018; Haffey et al., 2018), and post-fire climate  
67 including temperature and moisture conditions (Chappell, 1996; Meng et al., 2015; Stevens-  
68 Rumann et al., 2018; Kemp et al., 2019; Guz et al., 2021). Long-term assessment of post-fire  
69 vegetation recovery across forest types can offer valuable insights to researchers and land  
70 managers who seek to identify areas that could benefit from post-fire management and develop  
71 potential management actions such as fuels treatment, prescribed fire, carbon management, etc.

72 Several studies have documented vegetation recovery and associated biogeophysical and  
73 biogeochemical dynamics in response to wildfires by employing field-based observations  
74 including flux tower measurements (Chambers & Chapin III, 2002; Jin & Roy, 20005; Amiro et  
75 al., 2006; Randerson et al., 2006; Campbell et al., 2007; Dore et al., 2010; Kemp et al., 2016;  
76 Hankin et al., 2019; Ma et al., 2020), remote sensing observations (Veraverbeke et all., 2012;  
77 O'Halloran et al., 2014; Micheletty et al., 2014; Rogers et al., 2015; Bright et al., 2019; Vanderhoof  
78 et al., 2020), and modeling approaches driven by remote sensing observations (Hicke et al., 2003;  
79 Bond-Lamberty et al., 2009; Williams et al., 2012; Rogers et al., 2013; Maina et al., 2019). While  
80 instructive and critical for mechanistic understanding, local field-based studies on post-fire  
81 ecological dynamics tend to focus on small, localized areas, encompassing only a single or a few  
82 wildfire events (Meigs et al., 2009; Montes-Helu et al., 2009; Downing et al., 2019). In contrast,  
83 large-scale regional analyses using remotely sensed observations and modeling approaches tend  
84 to focus on Mediterranean (Veraverbeke et all., 2012a, 2012b; Meng et al., 2014; Yang et al.,  
85 2017) and boreal ecosystems (Amiro et al., 2000; Chambers & Chapin, 2003; Randerson et al.,  
86 2006; Lyons et al., 2008; Amiro et al., 2010; Jin et al., 2012; Rogers et al., 2013; Hislop et al.,  
87 2020), or on only a few forest types (mostly ponderosa pine and mixed conifer of western U.S.)  
88 (Chen et al., 2011; Dore et al., 2012; Meng et al., 2015; Roche et al., 2018; Bright et al., 2019;  
89 Littlefield et al., 2020). Moreover, such studies did not examine how their results scale up to  
90 multiple fire events across broad regions.

91 The purpose of this study is to provide a more precise estimate of wildfire impacts on LAI and  
92 surface albedo in seven different forest types of the western US using observations derived from  
93 the MODIS. Moreover, this study also examines the factors that influence the nature and rate of  
94 vegetation recovery in the post-fire environment. The hypotheses for the work are that 1) the rate

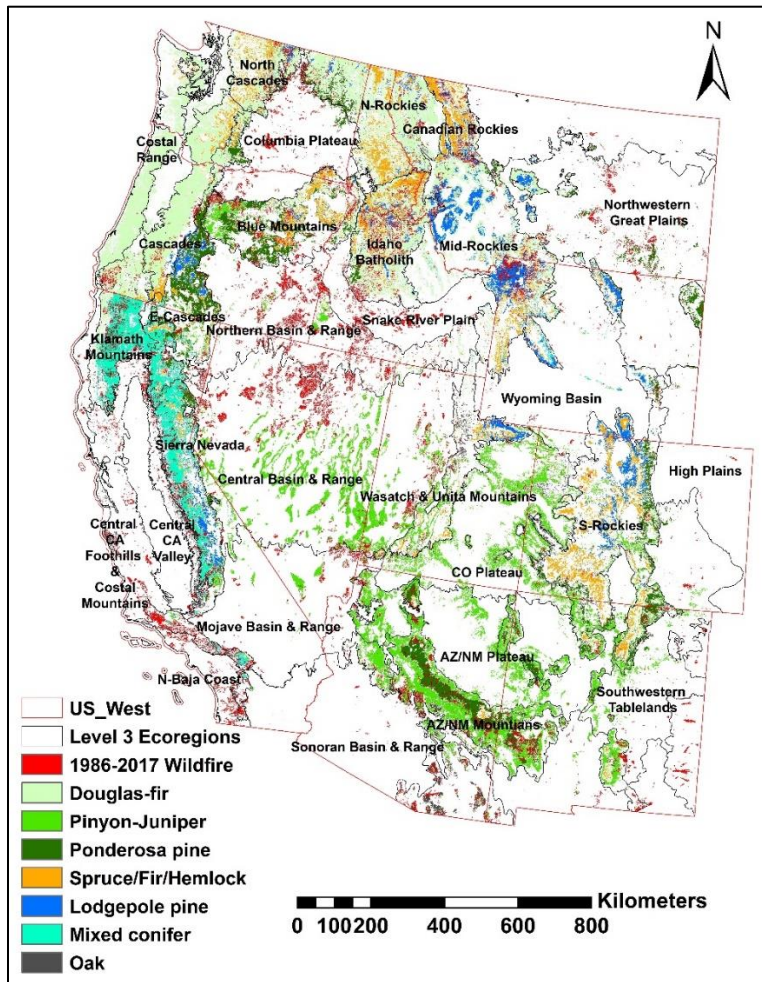
95 of recovery of LAI following wildfire varies across forest types and ecoclimatic settings, 2) the  
96 change in vegetation cover post-fire induces a change in the albedo which varies by forest types  
97 and ecoclimatic settings, and 3) the variability in the post-fire response of albedo is attributable to  
98 the same factors that explain variability in LAI post-fire.

99 **2. Methods**

100 **2.1. Study Area**

101 This study was carried out in the western US, a region that has been severely disturbed by wildfires  
102 in the last several decades. Its extent for the purpose of this study (Fig. 1) encompasses the  
103 conterminous US west of the 100<sup>th</sup> meridian (Thompson et al., 2003). This region is geographically  
104 diverse with high physiographic relief and strong local and regional climatic gradients (Bartlein &  
105 Hostetler, 2003), including regions such as temperate rain forests, high mountain ranges, great  
106 plains, and deserts (Thompson et al., 2003). Our study considered seven forest types that are  
107 dominant across the western US, as defined by the US Forest Service's National Forest Type data  
108 set (Ruefenacht et al., 2008), including Douglas-fir, Pinyon-Juniper, Ponderosa pine,  
109 Spruce/Fir/Hemlock, Mixed conifer, Lodgepole pine, and Oak. Within these forest types, we only  
110 considered areas that were burned with high severity as defined by Monitoring Trends in Burn  
111 Severity (MTBS) to examine the post-fire biophysical dynamics. In case of attribution of postfire  
112 recovery, we considered all fire severity classes from MTBS in our random forest model to  
113 determine the influence of these classes on post-fire recovery of vegetation and surface albedo.  
114 Within each ecoregion, we selected only those forest types that cover >10% of ecoregion's forest  
115 area and had >1% pixels burned under high severity. As a result, only 21 out of 35 level III  
116 ecoregions of the western US (Table S1) (Omernik, 1987) had a sufficient number of 500 m x 500  
117 m pixels that saw high severity burning within these forest types to support the generation of forest-

118 type-specific chronosequences of post-fire ecological responses. Across these ecoregions, average  
119 annual precipitation (1981-2010) was  $900 \pm 490 \text{ mm yr}^{-1}$  (mean  $\pm$  SD), while mean summer  
120 minimum and maximum temperature were  $23^\circ \pm 2.8^\circ\text{C}$  and  $7^\circ \pm 2.5^\circ\text{C}$ , respectively (PRISM; Daly  
121 et al., 2008).



122  
123 Figure 1: Distribution of 1986-2017 burned area (Eidenshink et al., 2007) and forest types  
124 (Ruefenacht et al., 2008) within study area extent.

## 125 2.2. Remote Sensing Data and Data Products

126 The burned area and fire severity data used in this study were obtained from Monitoring Trends in  
127 Burn Severity (MTBS) for the period of 1986-2017 (Eidenshink et al., 2007). We divided our study  
128 into different forest types to analyze the recovery of LAI and albedo post-fire, utilizing a USFS

129 forest type group map (Ruefenacht et al., 2008). We resampled the MTBS dataset from its native  
130 30 m resolution to a coarser 500 m resolution. During this process, we retained only those 500 m  
131 pixels that contained at least 75% of the corresponding 30 m pixels burned, thus reducing noise  
132 from pixels with an unclear mix of burn and unburn conditions. Similarly, we resampled forest  
133 type grid from 250 m to 500 m resolution and selected pixels where at least 75% of the forest  
134 within each pixel belonged to a single forest type based on the 250 m forest type group map. We  
135 excluded pixels that were burned more than once between 1986 and 2017 as such pixels can add  
136 noise to the post-fire trajectory of biophysical properties.

137 This study analyzed spatially and temporally consistent MODIS products: LAI and shortwave  
138 white sky albedo to assess fire-induced change in vegetation and surface albedo in the western US.  
139 The MODIS satellite data tile subsets (tiles h8v4, h8v5, h9v4, h9v5, h10v4, and h10v5) from 2001  
140 to 2019 were downloaded from the MODIS data archive (<https://www.earthdata.nasa.gov/>).  
141 Within each data tile, we employed the quality assurance (QA) bits embedded in the MODIS  
142 products to ensure that only the highest-quality values (flagged as '0') were included. This process  
143 involved removing all retrievals affected by cloud cover and those flagged for low quality. The  
144 MODIS LAI product (MCD15A2H; Myneni et al., 2002) reports the green leaf area index which  
145 represents the amount of one-sided green leaf area per unit ground area in broadleaf canopies or  
146 half the total surface area of needles per unit ground area in coniferous canopies. The MODIS LAI  
147 algorithm utilize a main look-up-table (LUT) based procedure that makes use of spectral  
148 information contained in red and NIR bands along with a back-up algorithm that relies on an  
149 empirical relationship between the Normalized Difference Vegetation Index (NDVI) and canopy  
150 LAI, and fraction of photosynthetically active radiation (fPAR) (Myneni et al., 2002).

151 For albedo, we used the daily MODIS collection 6 bidirectional reflectance distribution function  
152 (BRDF)/Albedo product at 500 m resolution (MCD43A3; Schaaf et al., 2002). The use of both  
153 Terra and Aqua data in this product provides more diverse angular samplings and increased  
154 probability of high input data that allow more accurate BRDF and albedo retrievals. The MODIS  
155 albedo algorithm uses a bidirectional reflectance distribution and shortwave reflectances (0.3-5.0  
156  $\mu\text{m}$ ) and provides both black-sky and white-sky albedos. We used shortwave broadband white sky  
157 albedo for this study because it is less biased in complex terrain and less sensitive to view and  
158 solar angles (Gao et al., 2005). We stratified the sampling of white-sky albedo by snow-free and  
159 snow-covered conditions based on the presence or absence of snow, determined at a pixel level by  
160 the MODIS daily snow cover 500 m product (MOD10A1; Salomonson and Appel, 2004). We  
161 assigned snow-free and snow-covered conditions using a threshold of less than 30% and greater  
162 than 75% snow cover. We chose these thresholds as a balance between inclusion for robust  
163 sampling and exclusion to reduce noise from pixels with an unclear mix of snow and snow-free  
164 conditions. We are aware that much of our study domain does not have considerable snow cover  
165 during winter, and these snow-free winter albedos had similar patterns and magnitudes as summer  
166 albedos (Fig. S1). Therefore, the average summer (June-August) albedo values presented here  
167 represent the snow-free condition only, while the average winter (December – February) values  
168 presented include only snow-covered conditions. We did not report winter albedos for all forest  
169 types because of limits on the availability of high-quality snow-covered pixels.

170 As part of our attribution analysis that seeks to identify factors that influence the pattern of post-  
171 fire biophysical dynamics, we acquired a suite of climate variables– monthly mean summer  
172 precipitation, monthly mean summer temperature, monthly minimum summer temperature,  
173 monthly maximum summer temperature, total annual precipitation– covering the 2001-2019

174 period from Parameter-Elevation Regressions on Independent Slopes Model (PRISM; Daly et al.,  
175 2008). PRISM utilizes point measurements of precipitation and temperature to generate continuous  
176 digital grid estimations for climate data with a 4 km spatial resolution (Daly et al., 1994). The  
177 elevation of all burned pixels was taken from the US Geological Survey (USGS) National  
178 Elevation Dataset (NED) at 30 m (U.S. Geological Survey, 2019). All topo-climatic variables were  
179 re-gridded to the 500 m MODIS resolution for uniformity.

180 **2.3. Generating Chronosequences of Post-fire LAI and Albedo**

181 To address unrealistic variation in MODIS land surface products (Cohen et al., 2006), we  
182 computed mean monthly values by adding all samples and dividing it by the number of samples  
183 in each month within our stratified design. For the summer season, we computed mean summer-  
184 season values of LAI and albedo by averaging the data from June, July, and August. Similarly, for  
185 the winter season, yearly values of LAI and albedo were computed the same way using data from  
186 December, January, and February. Next, we analyzed changes in post-fire LAI and albedo relative  
187 to pre-fire by sampling each of them as an annual time series from three years before wildfire  
188 events to all years of record after wildfire events. We grouped samples from each fire event based  
189 on forest type, eco-climatic setting, and snow cover conditions. Within these groups, we  
190 composited burn events from different years and aligned them temporally to represent three years  
191 prior to the fire and all years after the fire. Consequently, chronosequences of biophysical  
192 properties as a function of time since fire were created for a combination of seven forest types, two  
193 snow cover conditions (in case of albedo), and 21 sub-ecoregions.

194 **2.4. Attribution of Recovery**

195 We explored the relationships between albedo and LAI recovery and topo-climatic factors, and  
196 subsequently attributed the recovery at 10 years post-fire and 20 years post-fire using random  
197 forest (RF) algorithms, implemented in R (Breiman 2001; Liaw & Wiener, 2002). We used a non-  
198 parametric modeling method because most variable distributions were non-normal and RF does  
199 not require the variables to be normally distributed. Additionally, RF can handle tens of thousands  
200 of data points and provides variable importance scores. We initially selected seven explanatory  
201 variables - fire severity class (low, medium, and high), three temperature variables, two  
202 precipitation variables, and elevation. Although RFs do not require collinear variables to be  
203 removed (Breiman, 2001), we employed a Variance Inflation Factor (VIF) analysis for  
204 multicollinearity as a variable selection method to improve computation efficiency and enhance  
205 interpretation, particularly with respect to variable importance. VIF analysis involves: a)  
206 calculating VIF factors, b) removing the predictors from this set with  $VIF > 10$ , and c) repeating  
207 until no variable has  $VIF > 10$ . This provided us with four uncorrelated predictors to be used in the  
208 RF model - fire severity class, total annual precipitation, mean summer temperature (June –  
209 August), and elevation. We pooled post-fire LAI and albedo responses across 21 ecoregions within  
210 a given forest type for both time horizons (10-year post-fire and 20-year post-fire). The dataset  
211 was divided into training (80%) dataset to train the RF model and test (20%) dataset to validate  
212 the model. We created four RF models with 500 binary decision trees for each forest type (one for  
213 each time horizon for both LAI and albedo). We tuned the model to generate a model with the  
214 highest accuracy i.e., the lowest out-of-bag error among all tested combination of parameter  
215 values. The model's performance was assessed using the  $R^2$  metric. We used unscaled permutation  
216 accuracy instead of the traditional Gini-based importance metric to rank the relative importance  
217 among explanatory variables, as Gini-based importance was shown to be more strongly biased

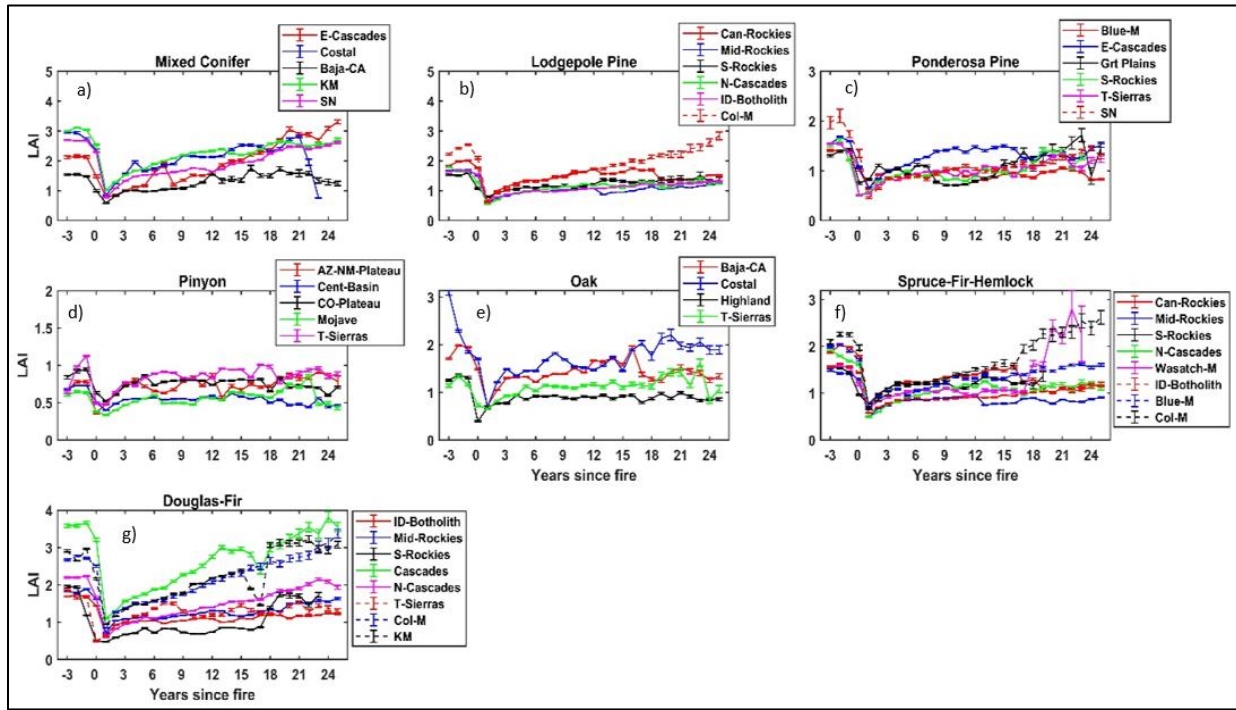
218 towards continuous variables or variables with more categories compared to other importance  
219 metrics (Strobl et al., 2007). The unscaled permutation importance metric calculates variable  
220 importance scores as the amount of decrease in the accuracy when a target variable is excluded.  
221 We used partial dependence plots (PDP) to visualize the influence of each explanatory variable on  
222 the degree of 10 years and 20 years post-fire recovery of LAI and albedo. PDP quantifies the  
223 marginal effects of a given variable on an outcome and provides a mechanism to explore insight  
224 in big datasets, especially when the random forest is dominated by lower-order interactions  
225 (Martin, 2014).

226 **3. Results**

227 **3.1. Post-fire Recovery of Land Surface Properties**

228 Burning caused a large decline in LAI for all forest types. Generally, high productivity forests  
229 (e.g., Douglas-fir and Mixed conifers), compared to other forest types, experienced a larger decline  
230 in LAI in year one after fire (Fig. 2a-g). Compared to pre-fire levels, the decline in LAI ranged  
231 from 47% in Pinyon-Juniper to 76% in Ponderosa pine forests (Table S2). After this initial  
232 decrease, the effects of vegetation regeneration became apparent. For all forest types, the  
233 magnitude of LAI change decreases with increase in time since fire. However, LAI did not recover  
234 to the pre-fire condition in most cases by the 25-year period of observation available for this study.  
235 We found large differences in the timing of LAI recovery across forest types, with forest types  
236 recovering at different rates, crossing the pre-fire levels at different times, and reaching different  
237 peaks in LAI (Fig. 2a-g). For example, Douglas-fir in Columbia Mountains, Klamath Mountains,  
238 and Southern Rockies (Fig. 2g) and Mixed conifers in Baja California and Eastern Cascades (Fig.  
239 2a) showed complete recovery of LAI to pre-fire levels within the 25-year study period, while  
240 Lodgepole pine, Oak, and Ponderosa pine were characterized by a slower recovery rate and most

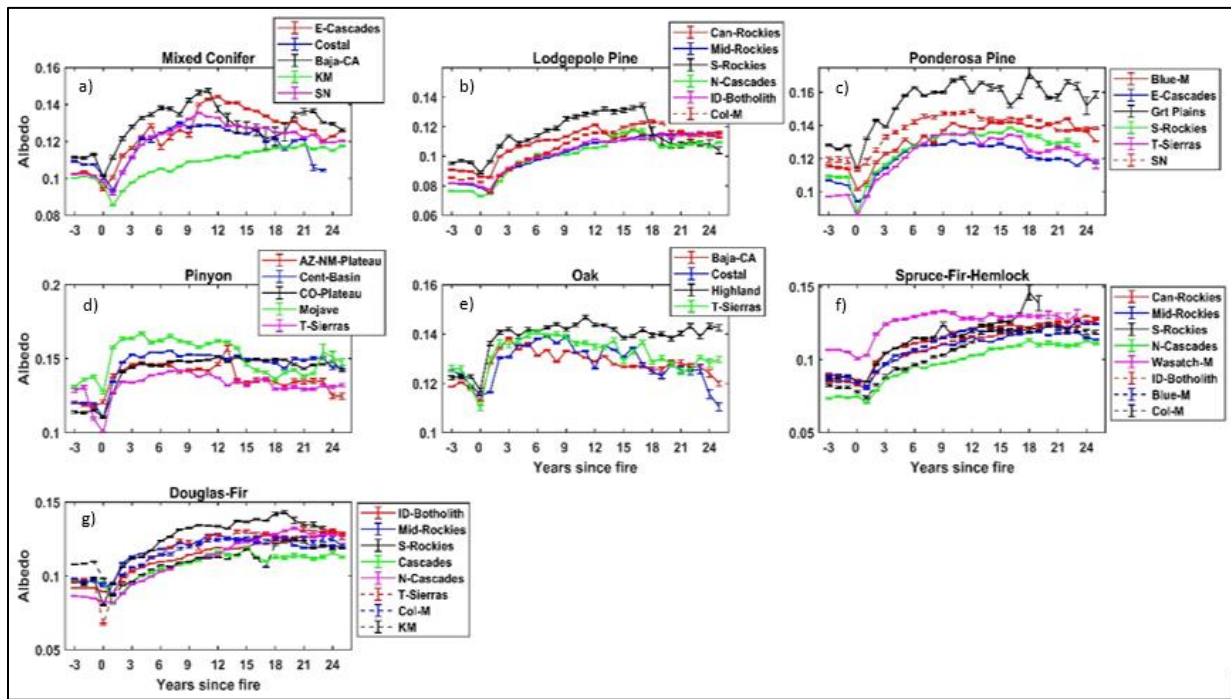
241 did not recover to pre-fire levels by the 25-year period (Fig. 2 and Table S2). We also found varied  
 242 recovery rates across geographic regions even within a single forest type, presumably related to  
 243 climate and soils. For example, the characteristic post-fire LAI trajectories for the high  
 244 productivity Douglas-fir forest type (Fig. 2g) showed a substantially faster recovery in Cascades,  
 245 Klamath Mountains, and Columbia Mountains regions compared to the Idaho Batholith region of  
 246 the western US. Based on observations from all forest types, in general, the faster recovery of LAI  
 247 was observed in high elevation, wet areas with substantial maritime influences.



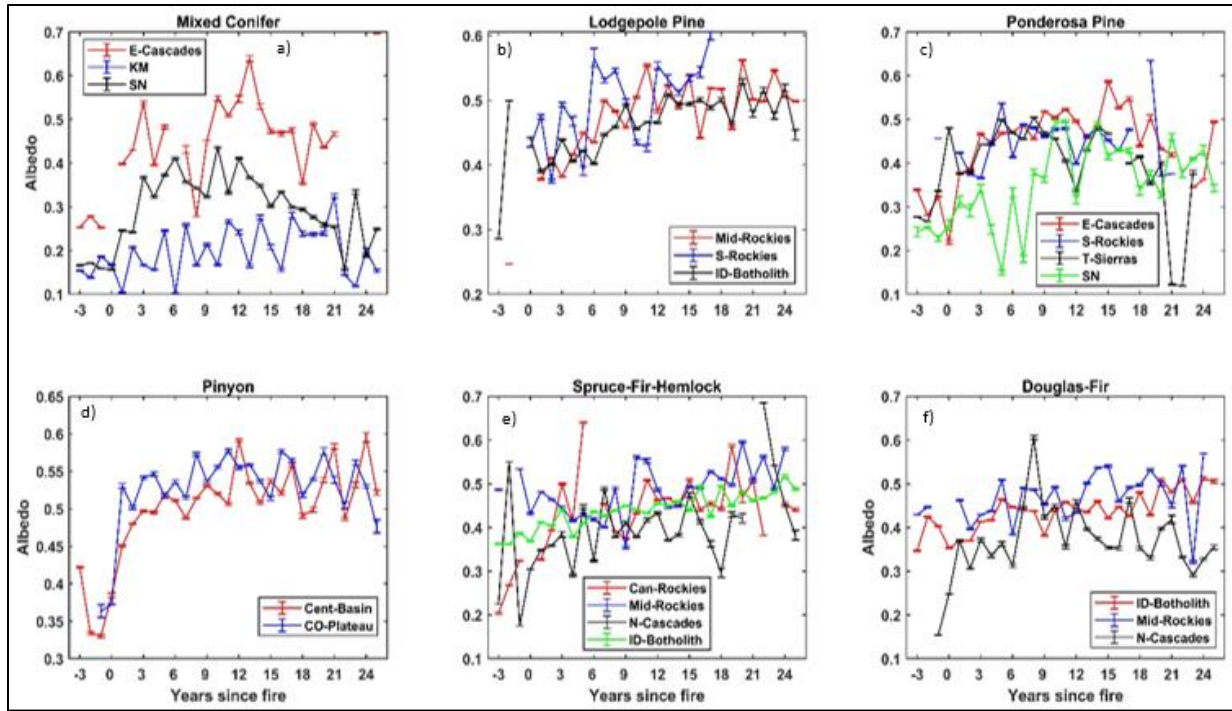
248  
 249 Figure 2: Mean summer post-fire LAI ( $\pm$  SE) as a function of time since fire in seven different  
 250 forest types of the western US. (Sub-ecoregions: E-Cascades = Eastern Cascades; Costal = Coastal  
 251 sage; Baja-CA = Baja California; KM = Klamath Mountains; SN = Sierra Nevada; Can-Rockies  
 252 = Canadian Rockies; Mid-Rockies = Middle Rockies; S-Rockies = Southern Rockies; N-Cascades  
 253 = Northern Cascades; ID-Batholith = Idaho Batholith; Col-M = Columbia Mountains; Blue-M =  
 254 Blue Mountains; Grt Plains = Great Plains; T-Sierras = Temperate Sierras; AZ-NM-Plateau =  
 255 Arizona-New Mexico Plateau; Cent-Basin = Central Basin; CO-Plateau = Colorado Plateau;  
 256 Mojave = Mojave Basin; Highland = North American Highland; Wasatch-M = Wasatch  
 257 Mountains).

258 Turning to albedo, we found significant changes in summer albedo post-fire of all forest types.  
259 Three important trends, similar among forest types, emerged from these post-fire summer albedo  
260 trajectories. First, for all forest types, summer albedo decreased immediately after fire (Fig. 3)  
261 likely due to low reflectivity by black carbon deposition on the soil surface and dead tree boles  
262 both common immediately after high severity burning. The decline in summer albedo ranged from  
263 0.01-0.02 across forest types with the greatest decline (20% from pre-fire levels; Table S3)  
264 observed in Douglas-fir forest of the Klamath Mountains region. Second, post-fire albedo  
265 increased gradually from year two since fire, crossing the pre-fire levels at around 3 years post-  
266 fire, and peaking at different time horizons for different forest types and regions (Fig. 3a-g).  
267 Elevated post-burn albedo is presumably due to increasing canopy cover, the relative high albedo  
268 of grasses and shrubs that establish in early succession, and the loss of black carbon coatings on  
269 soil and woody debris (Chambers and Chapin, 2002). The timing and magnitude of peak post-fire  
270 albedo varied across forest types. For example, Ponderosa pine showed its peak in post-fire albedo  
271 at 18 years post-fire (Fig. 3c) and 11 years post-fire for one of the Mixed Conifer regions (Fig. 3a),  
272 while slow growing species such as Spruce/Fir/Hemlock may not have reached its peak by the end  
273 of the 25-year post-fire study period (Fig. 3f). Similarly, there were significant regional differences  
274 in timing and magnitude of peak albedo for a given forest type group. For example, Mixed Conifer  
275 post-fire albedo peaked at 11 years post-fire in Baja California, while it continued to increase  
276 through to 25 years in Klamath Mountains (Fig. 3a). Third, as the post-fire LAI approached the  
277 pre-fire LAI levels, post-fire albedo started to decline from the peak towards its pre-fire albedo,  
278 but it did not reach the pre-fire albedo levels by the end of the 25-year study period (Fig. 3a-g).  
279 Post-fire winter albedo for each forest type had a similar pattern as summer albedo except with  
280 greater magnitude and that it increased immediately after fire (Fig. 4a-f and Table S4). We

281 observed greater inter-annual variability in the timeseries of post-fire winter albedo likely related  
 282 to variability in snow cover and also a smaller signal-to-noise ratio associated with smaller sample  
 283 sizes. The albedo response was more than three-fold larger in winter than in summer, peaking in  
 284 the range of 0.4 to 0.6 across forest types and with an increase over pre-fire levels of about 0.25 to  
 285 0.50. Similar to summer albedos, winter albedos did not return to the pre-fire levels by the end of  
 286 25-year study period (Fig. 4a-f).



287  
 288 Figure 3: Mean summer post-fire albedo ( $\pm$  SE) as a function of time since fire in seven different  
 289 forest types of the western US.



290

291 Figure: 4: Mean winter post-fire albedo ( $\pm$  SE) as a function of time since fire in seven different  
 292 forest types of the western US.

293 **3.2. Drivers of post-fire recovery of LAI and albedo**

294 Our random forest model had high accuracy for recovery of both LAI and albedo 10 years and 20  
 295 years post-fire. The out-of-bag (OOB) error rate of the random forest model for the relative  
 296 recovery of 10-year post-fire LAI was around 3% - 8% ( $r^2 = 0.66 - 0.78$ ), while it was around  
 297 2.5% - 9% ( $r^2 = 0.65 - 0.78$ ), 0.4% - 1.4% ( $r^2 = 0.55 - 0.83$ ), and 0.3% - 1.6% ( $r^2 = 0.52 - 0.83$ )  
 298 for 20-year post-fire LAI, 10-year post-fire albedo, and 20-year post-fire albedo, respectively  
 299 (Table S5). The variable with greatest importance agreed well between 10-year LAI and 20-year  
 300 post-fire LAI for all forest types indicating that the recovery of LAI at 10-year and 20-year post-  
 301 fire were both largely determined by the same governing factors (Fig. S2). Among all the  
 302 explanatory variables, the degree of post-fire LAI recovery at both 10-year and 20-year post-fire  
 303 were largely dominated by elevation and total annual precipitation (Fig. S2). In contrast, the factor  
 304 with greatest influence on post-fire summer albedo varied by forest type and time since fire. For

305 example, in the Mixed conifer forest type, annual precipitation was the major determinant of 10-  
306 year post-fire albedo recovery, while it was average summer temperature in case of 20-year  
307 postfire. Similarly, the degree of 10-year post-fire albedo recovery in the Spruce/Fir/Hemlock  
308 forest type was largely determined by average summer temperature, while the recovery after 20-  
309 year post-fire was mainly determined by elevation. Fire severity, on the other hand, showed almost  
310 no explanatory power in predicting recovery of LAI and albedo at both times for all forest types  
311 (Fig. S2,S3).

312 The degree of LAI recovery 10-year post-fire increased with an increase in total annual  
313 precipitation for all forest types, but it varied little when the total annual precipitation exceeded  
314 1000 mm. Annual precipitation was the major determinant of 10-year postfire LAI recovery for  
315 dry forests like Ponderosa pine, Pinyon-Junipers, and Oak, and these forest types tended to recover  
316 above pre-fire levels as the annual precipitation is increased. However, when the annual  
317 precipitation is less than 500 mm, the relative change in LAI is below 0 for all forest types,  
318 indicating that the complete recovery of LAI 10-year postfire was unlikely with annual  
319 precipitation less than 500 mm (Fig. 5c). In contrast, five out of seven forest types recovered over  
320 pre-fire levels 20-years post-fire with increased annual precipitation, indicating that Mixed  
321 conifers and Douglas-fir need more time and higher annual precipitation to recover to the pre-fire  
322 level. Only Oak and Ponderosa pine showed increased LAI 20-year post-fire as the annual  
323 precipitation exceeded 2000 mm (Fig. 6c). As with LAI, annual precipitation was one of the major  
324 determinants of both 10-year and 20-year post-fire albedo recovery. The post-fire increase in  
325 albedo was greater for sites with less annual precipitation (Fig. 7c and 8c), particularly noticeable  
326 in dry forest types such as Douglas-fir, Ponderosa pine, and Oak where increased precipitation  
327 triggered a rapid increase in post-fire vegetation recovery. The Oak forest type showed a particular

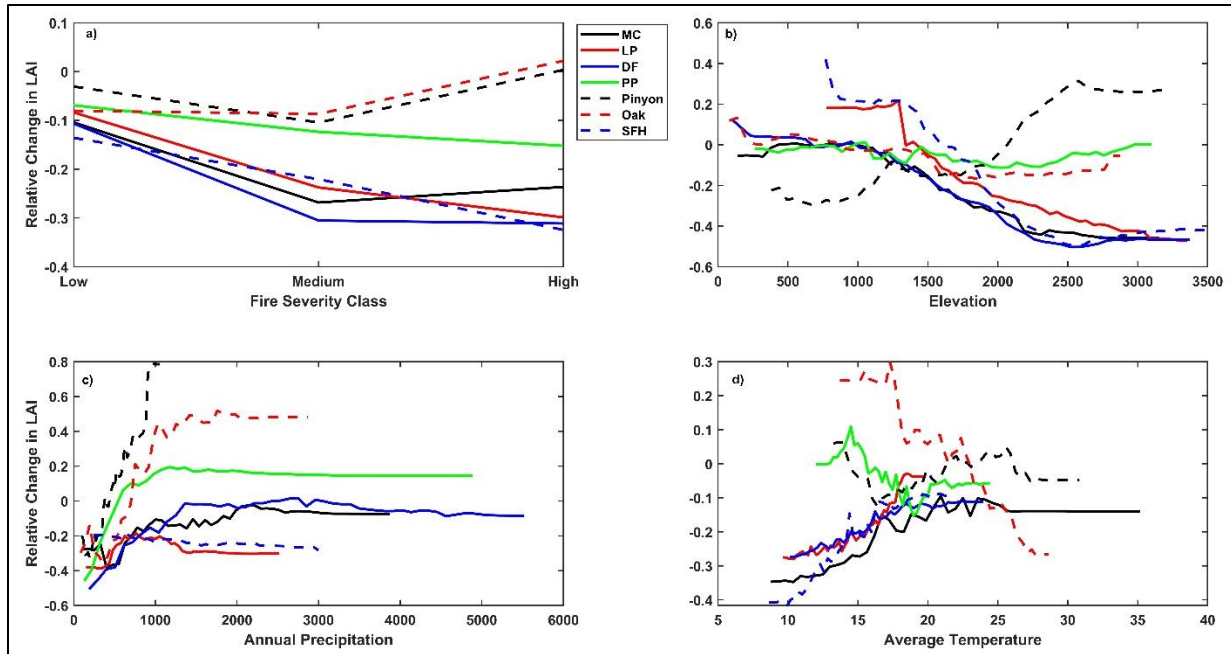
328 anomaly of albedo 20-years post-fire, exhibiting a decline of around 20% below pre-fire levels for  
329 sites with annual precipitation of 2000 mm or above (Fig. 8c), consistent with a rapid increase in  
330 vegetation recovery.

331 Regarding average summer temperature, we found interesting divergence in the pattern of LAI  
332 response between cool and hot climates. For forests growing in hotter conditions, the magnitude  
333 of LAI recovery at both time horizons decreased in areas with higher temperatures, particularly in  
334 Oak, Pinyon-Junipers, and Ponderosa pine forest types, as these forest types grow at warmer end  
335 of the species distribution. In contrast, increases in average summer temperature assisted the  
336 recovery of forest types growing at the colder end of the species distribution such as Lodgepole  
337 pine and Spruce/Fir/Hemlock (Fig. 5d and 6d), noting that LAI was consistently lower than pre-  
338 fire levels for these forest types at both time horizons. Albedo does not show the same divergence  
339 in pattern with warmer conditions, and instead we find a somewhat surprising pattern. Hotter sites  
340 tend to experience a larger enhancement of summertime albedo over the pre-fire condition at both  
341 time horizons in spite of faster recovery of LAI with hotter temperature (Fig. 7d and 8d).

342 Elevation was consistently found to be an important variable in determining the trajectory of post-  
343 fire vegetation recovery. The post-fire recovery of LAI was slower at higher elevation both 10-  
344 years and 20-years post-fire. Most forest types showed complete recovery towards pre-fire levels  
345 at an elevation below 1500 m. Only Pinyon-Junipers and Ponderosa pine forest types saw faster,  
346 more complete recovery of LAI with higher elevation (Fig. 5b and 6b). Turning to albedo response,  
347 we found that higher elevation led to a smaller increase in albedo over its pre-fire value for both  
348 time periods for the two forest types for which elevation was the most important predictor of post-  
349 fire albedo change, namely for Pinyon-Juniper and Ponderosa pine forests. This is consistent with  
350 faster post-fire recovery of LAI at higher elevation portions of range for these two forest types. In

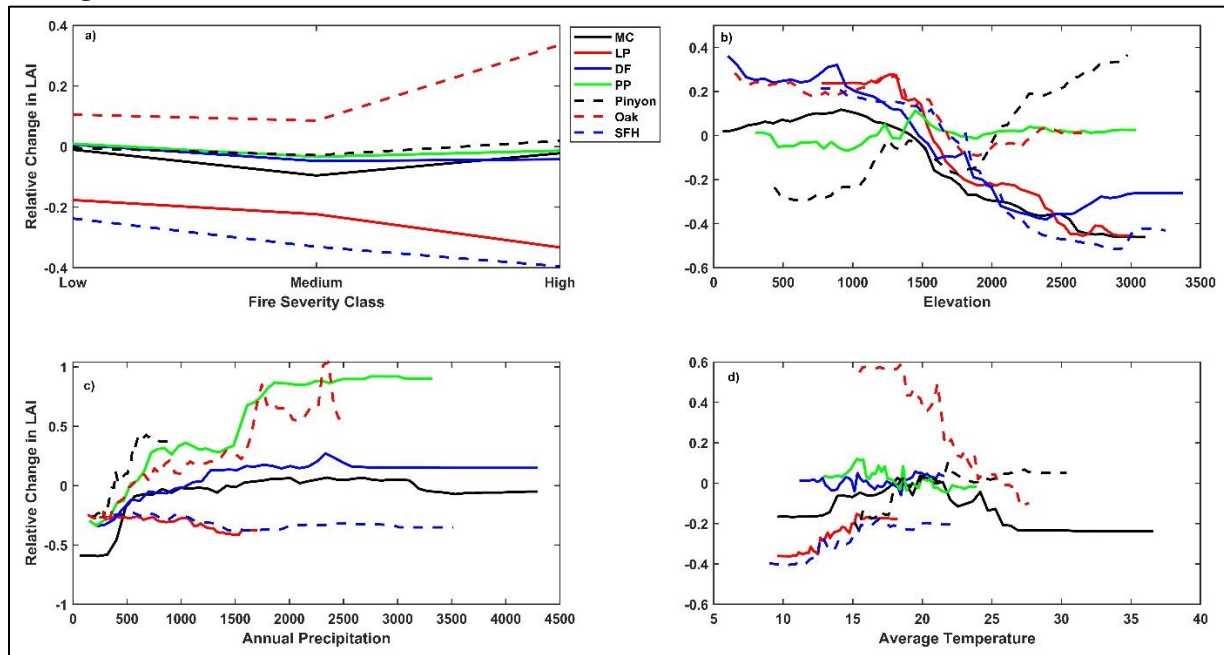
351 contrast, post-fire albedo of Douglas-fir, Mixed conifer and Oak forest types showed little  
352 dependence on elevation (Fig. 7b and 8b).

353 Although fire severity was the least important predictor of both post-fire LAI and albedo recovery  
354 at both time horizons, our results showed significant variation in post-fire recovery among severity  
355 classes for all forest types. As expected, the overall recovery of LAI 10-year post-fire was greater  
356 for low fire severity where the recovery ranged between 85% and 95% of pre-fire LAI levels (Fig.  
357 5a). Only in the case of Oak and Pinyon-Juniper forest types that burned with high severity did we  
358 see full recovery of LAI at or above pre-fire levels by 10-years post-fire. By 20 years post-fire,  
359 Lodgepole pine and Spruce/Fir/Hemlock still show a suppression of LAI relative to pre-burn and  
360 less recovery for more severe burn conditions (Fig. 6a) while Oak sees LAI elevated over the pre-  
361 burn condition and saw the largest LAI at sites that had the highest severity fires (Fig. 6a). The  
362 four other forest types had LAI equal to the pre-burn condition and showed no variation across fire  
363 severity. For albedo, all forest types showed a larger elevation of albedo over their pre-fire values  
364 under medium fire severity (Fig. 7a). Oak had the lowest change in albedo at both time horizons,  
365 owing to rapid post-fire recovery. Overall, post-fire albedo was consistently higher than pre-fire  
366 levels at both time horizons in all forest types indicating that albedo requires more than two  
367 decades to return to pre-fire levels in these forest types (Fig. 7a and 8a).



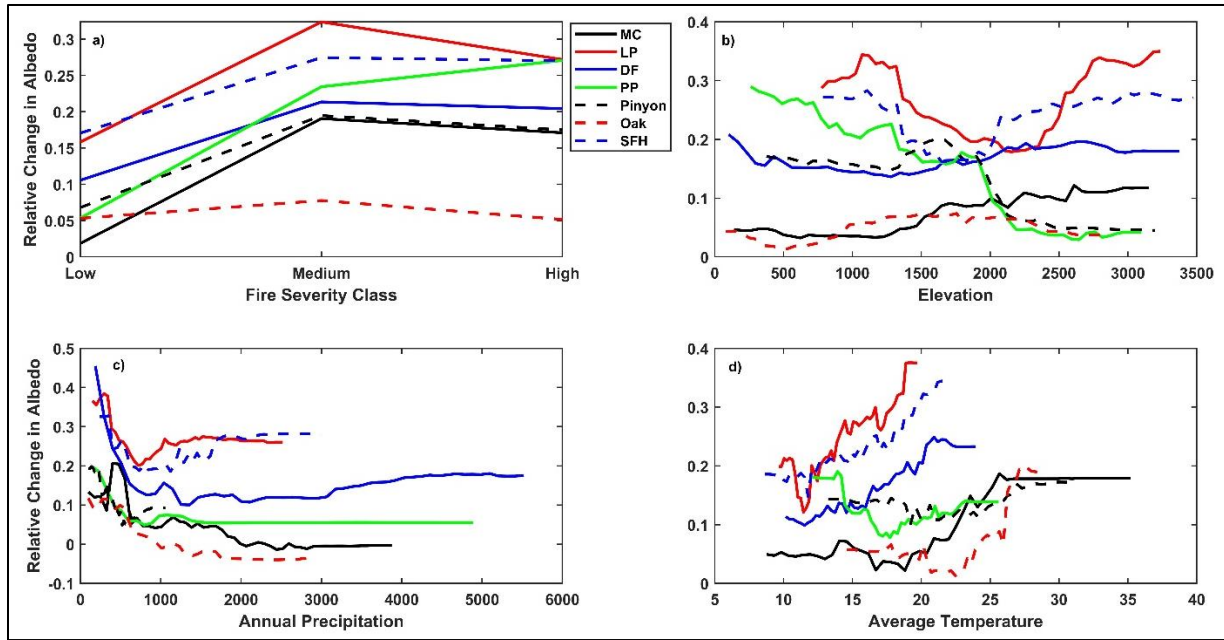
368  
369  
370  
371  
372  
373  
374  
375

Figure 5: Partial dependence of change in summer LAI 10-year post-fire relative to pre-fire on a) fire severity, b) elevation, c) annual precipitation, and d) mean monthly summer temperature. (Forest types: MC = Mixed Conifers; LP = Lodgepole pine; DF = Douglas-fir; PP = Ponderosa pine; Pinyon = Pinyon-Juniper; SFH = Spruce/Fir/Hemlock). The y-axis represents change in LAI post-fire relative to pre-fire (degree of recovery), where negative values represent recovery below pre-fire levels, 0 represents recovery to pre-fire levels, and positive values represent recovery above pre-fire levels.



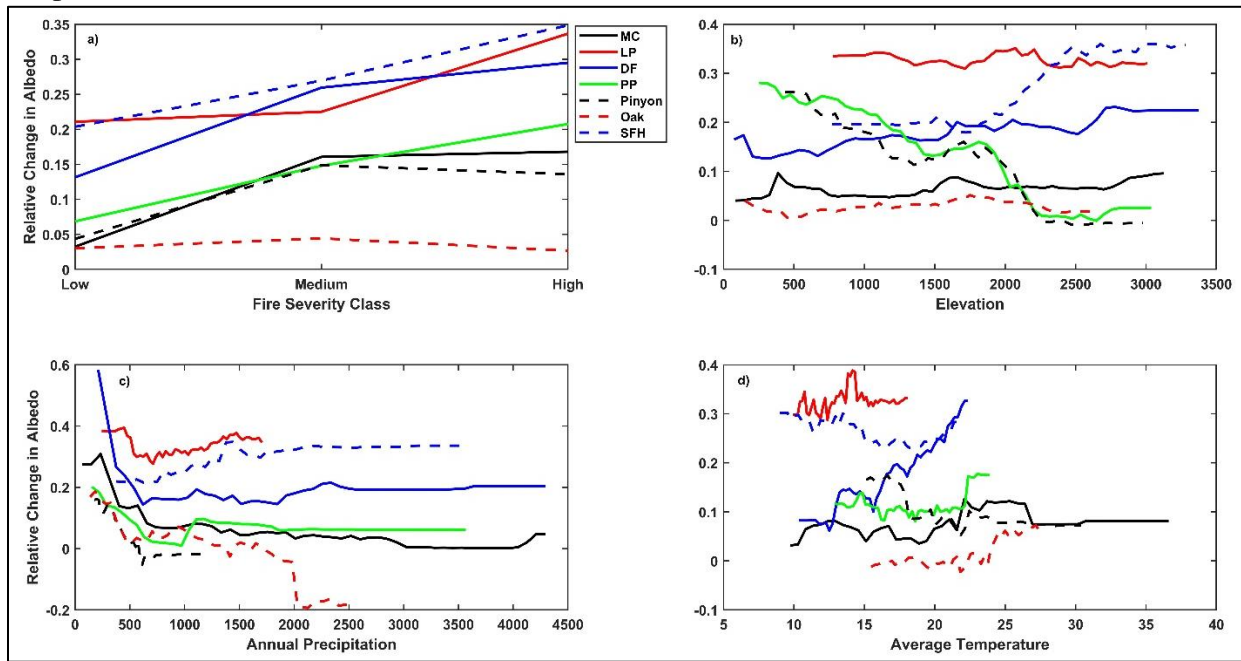
376  
377  
378

Figure 6: Partial dependence of change in summer LAI 20-year post-fire relative to pre-fire on a) fire severity, b) elevation, c) annual precipitation, and d) mean monthly summer temperature.



379  
380  
381  
382

Figure 7: Partial dependence of change in summer snow-free albedo 10-year post-fire relative to pre-fire on a) fire severity, b) elevation, c) annual precipitation, and d) mean monthly summer temperature.



383  
384  
385  
386

Figure 8: Partial dependence of change in summer snow-free albedo 20-year post-fire relative to pre-fire on a) fire severity, b) elevation, c) annual precipitation, and d) mean monthly summer temperature.

387

#### 4. Discussion and Conclusion

388 Here, we extended the regional research by Shrestha et al., (2022) with a much broader sampling  
389 to study post-fire responses for seven forest types in 21 sub-ecoregions of the western U.S. In  
390 addition, this study also uses a machine learning approach (random forest) to examine the influence  
391 of several topo-climatic variables on the nature and rate of vegetation recovery and associated  
392 albedo in the post-fire environment.

393 **4.1. Post-fire Vegetation Recovery**

394 In this study, we used MODIS-derived LAI to increase our understanding of variability in the  
395 recovery of vegetation in the post-fire environment across seven forest types and 21 sub-  
396 ecoregions of the western United States. Similar to other studies (Morresi et al., 2019; Vanderhoof  
397 et al., 2020), we found rapid vegetation recovery in the first 10 years after fire. While LAI  
398 rebounded rapidly in the initial 10 years post-fire, this cannot be taken as a definitive indicator of  
399 successional trajectory, especially for slow growing forests like subalpine fir (Ferguson and  
400 Carlson, 2010) or for forests with episodic post-fire germination such as Ponderosa pine (Savage  
401 et al., 1996; Brown and Wu, 2005; Rodman et al., 2019). Leaf area recovery then slowed in most  
402 cases, and for many it did not return to the pre-fire level by the end of study period. We anticipate  
403 that the recovery of LAI to its pre-fire condition continues to unfold over time, extending beyond  
404 the 25-year duration covered by our study. In some cases, we see LAI at 20 or 25 years post-fire  
405 exceeding that prior to burning, suggesting that wildfire may have stimulated canopy renewal or  
406 release of the understory. Evaluating post-fire LAI trajectories on these, and longer, timescales can  
407 be of value from a management perspective, for example, to identify regions where there is a risk  
408 of regeneration failure for dominant, native species (Welch et al., 2016).

409 Our findings demonstrated differences in characteristic trajectories across forest types and  
410 ecoregions. Wildfire caused a similar proportional reduction of LAI across forest types and

411 ecoregions, generally with 30% to 70% reduction in year 1 post-fire but with smaller reductions  
412 in some Pinyon-Juniper setting (Table S2). We also found varied rates of LAI recovery post-fire  
413 across forest types and ecoregions. Some forest types saw recovery to only 60 % to 70% by 25  
414 years while others saw LAI recovery to 120% to 150% of the pre-fire condition (Table S2). Many  
415 factors are likely to contribute to these patterns across forest types and ecoclimatic settings. First  
416 and foremost, it is no surprise that areas more suitable for growth have faster and more complete  
417 recovery with higher absolute LAI within a given forest type. For example, Douglas-fir stands in  
418 Cascades, Columbia Mountains, and Klamath Mountains had faster recovery rates and greater  
419 changes in absolute LAI after year 1 post-fire than did stands in the Rockies and Temperate Sierras  
420 (Table S2). Similarly, we observed a consistent slow trend in the rate of conifer regeneration in  
421 the interior of the western US with continental climate where high severity fire is common. This  
422 is likely due to reduced seed availability in response to larger high severity fires in these areas.  
423 (Cansler and McKenzie, 2014). Other factors include the regeneration capacity of the dominant  
424 tree species post-fire, with some readily and actively resprouting or having serotiny, while other  
425 lack these fire-adaptation traits (Howard, 2003; Meng et al., 2018), and competition with species  
426 such as early colonizers common after burning (Hansen et al., 2016; Stoddard et al., 2018). The  
427 post-fire dynamics presented here are not stratified by post-fire species composition, only  
428 characterizing the biophysical characteristics that unfold after burning of a particular forest type.  
429 Naturally, post-fire species composition can differ from pre-fire depending on seed and nutrient  
430 availability, fire severity, and climate and these effects are embedded in the post-fire biophysical  
431 trajectories that we present. Further exploration of how post-fire species composition and other  
432 regeneration characteristics influence biophysical trajectories is warranted.

433 Our findings of post-fire LAI trajectories across ecoclimatic settings suggest that the range of  
434 Douglas-fir stands may be less limited due to climate warming compared to Ponderosa pine, as  
435 their current range tends to extend into cooler and moister areas where they recover above pre-fire  
436 levels. This indicates that the worsening of climate changes in the future (more periods of  
437 prolonged drought) can have implications for migration of ponderosa pine due to worsening  
438 regeneration under climate stress. Although Pinyon-Juniper forests recovered rapidly in the first  
439 few post-fire years, our observed decline in the rate of pinyon-juniper recovery is consistent with  
440 the findings of Vanderhoof et al., (2020). This forest type is recognized for its slow regeneration  
441 and susceptibility to drought (Hartsell et al., 2020). Existing studies in post-fire recovery of  
442 Pinyon-Juniper suggest that this forest type recovers to pre-fire condition in <5 years after fire in  
443 the case of low to moderate fire (Jameson, 1962; Dwyer and Preper, 1967), while it takes >100  
444 years for recovery to pre-fire condition under high severity with heavy Pinyon-Juniper mortality  
445 (Erdman, 1970; Koniak, 1985). Other forest types showed faster or similar rates of recovery, for  
446 instance, Mixed conifer recovered completely in most of the ecoregions of the western US possibly  
447 due to richer species diversity and relatively higher precipitation (Bright et al., 2019).

448 **4.2. Post-fire albedo Changes**

449 Our results provide evidence for significant effects of wildfires on the albedo across forest types  
450 and eco-climatic settings in the western US, with post-fire albedo being much higher in winter  
451 than in summer. All forest types showed noticeable age-dependent albedo patterns, with a transient  
452 peak in summer albedo around 10-18 years post-fire. We observed a decline in summer albedo  
453 during the first year after fire except for Pinyon-Juniper (Table S3) presumably from charred  
454 surface and the deposition of black carbon. The increase in albedo in first year after fire in Pinyon-  
455 Juniper may be associated with low pre-fire LAI leading to lower levels of charcoal and black

456 carbon deposition that absorb incoming radiation. Our finding is comparable to previously  
457 published findings that report albedo drops in the range of 0.01-0.05 using MODIS albedo (Jin and  
458 Roy, 2005; Randerson et al., 2006; Lyons et al., 2008; Veraverbeke et al., 2012). The slight  
459 differences are likely related to the variability in the domain of each study (e.g., western US vs.  
460 boreal, western US vs. Mediterranean), spatial resolution of MODIS pixels (500 m) that includes  
461 unburned patches and non-forest fractions, illumination conditions of the MODIS albedo products  
462 (black sky, white sky, blue sky) and method used to calculate albedo differences. Regarding the  
463 latter, we compared a pixel to itself between pre-and-post-fire years. The approach of comparing  
464 burned pixels to unburned neighboring pixels as control is also common (e.g., Myhre et al., 2005;  
465 Randerson et al., 2006; Lyons et al., 2008; Gatebe et al., 2014). One issue with this approach is  
466 that it does not consider heterogeneity of the land surface. Burned and control pixels may not be  
467 equivalent in the pre-burn period (Dintwe et al., 2017), as they do not necessarily represent a  
468 comparable vegetation state and therefore may not be a good proxy to pre-fire state.

469 Soon after fire, we observed an increased in post-fire albedo during the summer period presumably  
470 due to combination of char removal and presence of early-successional plants (Johnstone et al.,  
471 2010) that have higher albedo than mature species (Betts and Ball, 1997; Pinty et al., 2000; Amiro  
472 et al., 2006; Dintwe et al., 2017). Summer post-fire albedo recovered faster than LAI regardless of  
473 vegetation type. This pattern suggests that, in contrast to findings of Pinty et al., (2000) and  
474 Tsuyuzaki et al., (2009), post-fire recovery of albedo is driven by multiple factors in addition to  
475 the early regeneration of vegetation such as vegetation destruction and charcoal left behind (Jin et  
476 al., 2012), differences in fuel combustion and consumption (Jin and Roy, 2005), species  
477 composition during early succession (Beck et al., 2011), and seasonal variation in soil moisture  
478 and removal of black carbon (Montes-Helu et al., 2009; Veraverbeke et al., 2012). As the

479 regenerating vegetation matures, the increase in post-fire albedo progressively weakens as  
480 suggested by Amiro et al., (2006), reaching peak at ~ 10-18 years post-fire which then gradually  
481 decline towards pre-fire levels. We did not observe the complete recovery of post-fire albedo  
482 within the study period of 25 years post-fire. Many studies using remote sensing technique suggest  
483 that albedo in post-fire stands commonly equilibrates at ~40-80 years post-fire (Randerson et al.,  
484 2006; Lyons et al., 2008; Kuusinen et al., 2014; Bright et al., 2015; Abdul Halim et al., 2019, Potter  
485 et al., 2020).

486 We found the greatest increase in post-fire albedo during winter, a finding consistent with others  
487 (Liu et al., 2005; Randerson et al., 2006; Montes-Helu et al., 2009; Gleason et al., 2019) due to  
488 increased exposure of snow resulting from the loss of canopy and tree mortality. In our analysis,  
489 post-fire winter snow-covered albedo increased with time since fire until a peak was reached, the  
490 timing of which varied across forest types. We hypothesize that this increase with time may result  
491 from the fall of standing dead snags (O'Halloran et al., 2014) and lower rate of reestablishment  
492 during succession (Fig. S4). Our finding showed similar post-fire winter albedo patterns across  
493 forest types in a region. For example, winter albedo in Lodgepole pine, Spruce/Fir/Hemlock, and  
494 Douglas-fir forest types in the Idaho Batholith region increased at a similar rate with time since  
495 fire which corresponds to consistent lower LAI recovery rate across these forest types in this region  
496 (Fig. S4b,f,g). However, variation in winter albedo was greater across ecoregions within a forest  
497 type (e.g., Mixed conifer) owing to variable rates of post-fire LAI recovery (Fig. S4a). Overall,  
498 our findings indicate a strong dependency of post-fire seasonal albedo on the proportion of  
499 vegetative cover, irrespective of forest types, on the post-fire environment. This observed effect  
500 provides a strong connection between albedo and successional patterns observed in these specific  
501 forest types.

502      **4.3. Controls on post-fire recovery of biophysical parameters**

503      One of the major contributions of our approach is that it not only generates the post-fire trajectories  
504      of land surface biophysical properties across a range of forest types and geographic regions, but  
505      also distinguishes the contribution of nature of fire, climate, and topography on post-fire LAI and  
506      albedo recovery for each forest type. Previous work has shown fire severity to be an important  
507      driver of regeneration (Crotteau et al., 2013; Meng et al., 2015; Chambers et al., 2016; Vanderhoof  
508      et al., 2020). In contrast, our analysis suggested fire severity was of relatively low importance  
509      relative to other variables considered (Fig. S2). Despite being of lesser importance, we found that  
510      higher rates of post-fire recovery were associated with low severity fire and lowest recovery rates  
511      were associated with high fire severity. The lower recovery rates associated with high fire severity  
512      are possibly due to lower seed availability and greater distance to live seed sources (Haire &  
513      McGarigal, 2010; Kemp et al., 2016; Kemp et al., 2019), but high fire severity can also create  
514      mineral seed beds and free up essential resources such as moisture, light, and nutrients which  
515      promote the growth of vegetation (Gray et al., 2005; Moghaddas et al., 2008). Only Oak and  
516      Pinyon-Juniper showed higher recovery rates under high fire severity among forest types which is  
517      primarily due to rapid regeneration by resprouting in Oak (Meng et al., 2018) and colonization by  
518      resprouting shrubs in Pinyon-Juniper (Wangler & Minnich, 1996). The low importance of fire  
519      severity in determining post-fire vegetation growth indicates that the variability across a single fire  
520      may be outweighed at a regional level by climate and its proxies. It also suggests that at some sites,  
521      the impact of wildfire may be restricted to causing tree mortality under changing climate, rather  
522      than also significantly influencing the post-fire regeneration with its impact on seed availability  
523      (Kemp et al., 2019).

524 Our analysis indicated that among all the factors considered, elevation had the highest variable  
525 importance score in predicting the LAI 10-year and 20-year post-fire. We found greater rates of  
526 vegetation recovery in lower elevation. Less successful recovery at higher elevations is likely  
527 associated with cooler temperatures at higher elevations for many of the forest types, and those  
528 cool temperatures appear to still limit forest establishment and growth, even under general  
529 warming in the region (Stevens-Rumann et al., 2018). Only Pinyon-Juniper showed increased  
530 recovery with elevation (Fig. 5b and 6b) likely due to relief from the hot, dry conditions at lower  
531 elevations but also possibly due to resistance to invasion that increases with elevation in this forest  
532 type (Urza et al., 2017), suggesting that warming temperatures are having a detrimental effect on  
533 post-fire regeneration at warmer sites, but not yet promoting post-fire regeneration at cooler sites  
534 at all spatial scales (Harvey et al., 2016). Elevation was found to be important in various studies  
535 of post-fire regeneration of conifer forests in the western U.S., but with opposite directionality  
536 (Casady et al., 2010; Rother & Veblen, 2016; Vanderhoof et al., 2020). However, Mantgem et al.,  
537 (2006) reported a strongly negative correlation with seedling density of Mixed conifer forests in  
538 the Sierra Nevada. In higher elevation forests such as Lodgepole pine, most studies demonstrated  
539 increased recovery post-fire (e.g., Harvey et al., 2016) which contrasted with our findings. These  
540 findings collectively highlight that there exists a large degree of uncertainty around individual  
541 forest type responses to post-fire climatic variability.

542 Our study adds to a growing body of literature emphasizing the importance of climate for post-fire  
543 vegetation growth among different forest types (Meng et al., 2015; Buechling et al., 2016; Rother  
544 and Veblen, 2017; Hankin et al., 2019; Vanderhoof et al., 2020). Our data suggests that high  
545 average summer temperatures and low water availability limit the recovery of LAI 10-year and  
546 20-year postfire on these forest types. Drier forests such as Oak, Ponderosa pine, Douglas-fir, and

547 Pinyon-Juniper were strongly associated with annual precipitation and mean summer temperature,  
548 which is consistent with the findings of Meng et al., (2015) and Kemp et al., (2019). Our analysis  
549 also suggests that the critical thresholds for annual precipitation and mean summer temperature  
550 are 500 mm and 15-20°C, respectively, in these forest types. Our finding of higher sensitivity of  
551 Oak, Ponderosa pine, Douglas-fir, and Pinyon-Juniper to annual precipitation and average summer  
552 temperature suggests that future increases in temperature and water deficit may affect these forest  
553 types more so than other forest types. With a trend toward warmer springs and summers in recent  
554 decades throughout the western US (Westerling, 2006; Ghimire et al., 2012; IPCC, 2013; Williams  
555 et al., 2021), conditions for post-fire vegetation growth and survival are changing, as even a slight  
556 increase in water deficit on the drier sites can have adverse effects on tree regeneration (Stevens-  
557 Rumann et al., 2018). While warming temperature has been shown to affect the post-fire  
558 regeneration of conifer forests growing at the warmer end of the species distribution such as  
559 Douglas-fir and Ponderosa pine (Haffey et al., 2018; Kemp et al., 2019), it could promote the rate  
560 of post-fire recovery for conifer forests growing at the colder end of the species distribution  
561 previously limited by frozen soils, cold temperatures, and snow (Stevens-Rumann et al., 2018;  
562 Vanderhoof et al., 2020).

563 Similar to LAI, our results of variable importance in random forests showed low importance of  
564 fire severity compared to other variables in post-fire recovery of summer albedo at both time  
565 horizons (Fig. S3). However, we noticed a difference in albedo change across fire severity classes.  
566 For example, we found lower albedo values in low fire severity areas compared to medium and  
567 high severity areas at both time horizons, which is associated with a greater degree of LAI recovery  
568 in low severity areas as vegetation has lower albedo than bare areas. Moreover, lower albedo 10-  
569 years post-fire in high severity compared to medium severity could be due to standing snags

570 absorbing sunlight, with it taking 5-15 years for just half of dead snags to fall (Russell et al., 2006).  
571 We did not find significant impact of elevation on post-fire albedo change in these forest types  
572 except for Pinyon-Juniper and Ponderosa pine, which showed decreased albedo post-fire in  
573 response to increased LAI with elevation. As expected, climate, particularly annual precipitation,  
574 was the major determinant of post-fire albedo change. Annual precipitation was found to be highly  
575 associated with changes in post-fire albedo in all forest types, where increased precipitation  
576 decreased the albedo post-fire with impact more prominent in 20-year post-fire. Annual  
577 precipitation impacts post-fire albedo through two different mechanisms. First, increased annual  
578 precipitation is associated with greater recovery of LAI in these forest types (Fig. 6c) where the  
579 mid-age stands replace the initial post-fire establishments, reducing albedo (Chambers and Chapin,  
580 2002). Second, soil moisture depends on precipitation. With greater precipitation leading to  
581 increased soil water content, we could expect a corresponding decrease in albedo due to darkening  
582 of soil particularly in open canopy conditions where the soil received direct radiation (Montes-  
583 Helu et al., 2009). Furthermore, an increase in leaf area within the understory during the wet season  
584 could have a similar effect, as reported in Thompson et al. (Thompson et al., 2004). Regarding  
585 temperature, the pattern of albedo recovery did not correspond well with the pattern of LAI  
586 recovery at both time horizons in these forest types. Albedo is elevated over the pre-fire condition  
587 more in the warmer part of a forest type's range even in forest types that have a faster recovery of  
588 LAI in that warmer domain. We might expect that a higher LAI would be associated with a lower  
589 albedo, but evidently the association is not as simple, and it might have something to do with  
590 species composition rather than simply leaf area. Our results point to the importance of climate  
591 patterns as a driver of post-fire summer albedo recovery through their influence on ecological  
592 succession on the post-fire environment.

593      **4.4. Significance and limitations of our Analysis**

594      Our results should be interpreted in light of four constraints. First, the accuracy of MODIS product  
595      algorithm is dependent on biome-specific values, which following extensive fire-caused mortality,  
596      can introduce additional uncertainty due to assumption of fixed land cover type. In addition, we  
597      utilized the recovery of MODIS LAI as an indicator of vegetation recovery. One significant  
598      limitation of LAI-based analysis is that it captures some of the aggregate effects of mortality and  
599      regrowth but does not fully characterize shifted species composition and community structure on  
600      the ground. Therefore, detailed, intensive field monitoring of vegetation structure both before and  
601      after fires can serve as a valuable complement to LAI-based analysis (Williams et al., 2014).  
602      Additionally, incorporating additional remote observations at the species level from the fusion of  
603      very high spatial resolution, lidar, or hyperspectral data (Huesca et al., 2013; Polychronaki et al.,  
604      2013; Kane et al., 2014) can further enhance the assessment. Second, in terms of albedo, we used  
605      a 500 m MODIS albedo product which reflects a somewhat larger area (Campagnolo et al., 2016).  
606      Each 500 m grid may in fact include a mix of burned and unburned patches which could result in  
607      underestimation of post-fire albedo. Although the use of MODIS data with its relatively low spatial  
608      resolution will miss some of the details of fine-scale spatial variability in burn severity, land cover  
609      type and so forth (Key, 2006), MODIS data has advantages in terms of higher temporal frequency  
610      of sampling that can be important in post-fire biophysical dynamics (Lhermitte et al, 2010;  
611      Veraverbeke et al., 2010, 2012) and these data also have good temporal coverage going back  
612      decades. Furthermore, higher resolution datasets on biophysical properties are still not  
613      operationally available. Third, the quality of our results may be constrained by the accuracy of fire  
614      severity from the MTBS product as dNBR is not a perfect metric of severity and may struggle to  
615      capture some variations in severity (Roy et al., 2006; De Santis and Chuvieco, 2009). However,

616 several new generation fire remote sensing products (Csiszar et al., 2014; Parks et al., 2014;  
617 Boschetti et al., 2015) are emerging in recent years, which hold the potential for further  
618 improvements in post-fire recovery studies. Finally, post-fire vegetation recovery in burned areas  
619 may vary from one location to another, influenced by several other factors that this study did not  
620 cover. To gain a comprehensive understanding of the trajectory of post-fire vegetation recovery,  
621 future studies, in addition to topo-climatic variables, should consider species competition,  
622 scorching of the seed bank, distance to seed tree, other post-fire disturbances, physiology of cones,  
623 seeds, and seedlings, as well as the interactions among all influencing drivers in these settings.

624 Despite these limitations, by aggregating across multiple fire events in 21 different sub-ecoregions  
625 and arraying observations along a 25-years chronosequence, our results demonstrate the spatial  
626 and temporal variability of fire effects on post-fire environment. Understanding such variability of  
627 fire effects and vegetation in space and time is important for comprehensive understanding of the  
628 drivers of natural regeneration and vegetation recovery in post-fire environments (Stevens-  
629 Rumann and Morgan, 2019). Our analysis could also help improve the modeling of post-fire  
630 recovery pathways by identifying the most important predictors of post-fire recovery and by  
631 approximating related thresholds of response. For example, our results suggest a full recovery of  
632 LAI in dry, low elevation forest types like Pinyon-Juniper, Ponderosa pine, and Oak within 10  
633 years post-fire when the annual precipitation exceeds the threshold of 500 mm and average summer  
634 temperature is  $\sim$ 15-20°C. A quantitative measure of primary controls is needed if efforts to develop  
635 realistic post-fire LAI trajectories for ecohydrological modeling studies are to be successful, as  
636 suggested by McMichael et al., (2004).

637 One major significance of our approach and findings is its potential to advance the land surface  
638 models (LSMs) embedded in Earth system models (ESMs). Currently, these models lack robust

639 representations of the ecological and biophysical consequences resulting from wildfire events  
640 (Lawrence and Chase, 2007; Williams et al., 2009). Modelers could use the pattern of post-fire  
641 biophysical dynamics as a function of time since fire, emerged from our data analysis, to inform  
642 the LSMs to more accurately represent biophysical and ecological functions of severely disturbed  
643 landscapes.

644 **4.5. Implications of Our Research**

645 There is mounting evidence of increased extreme fire incidents in the western US due to ongoing  
646 climate change (Westerling et al., 2006; Williams et al., 2014), leading to rapid alteration and  
647 considerable uncertainty regarding species composition (McDowell et al., 2015) and ecological  
648 dynamics (Johnstone et al., 2016). This study provides an estimate of the effect of the post-fire  
649 environment on vegetation and surface albedo balance of the western US. The chronosequence  
650 data show clear patterns with time since fire for both biophysical parameters. Our results show that  
651 conifer forest ecosystems, particularly Douglas-fir and Ponderosa pine, are slower to recover post-  
652 fire, which may indicate they face greater risks from the projected increase in fire severity and  
653 frequency as forecasted for drier interiors of the western US (Abatzoglou and Williams, 2016;  
654 Littell et al., 2018). The post-fire biophysical changes documented here could be of significance  
655 for local to regional climates, potentially eliciting feedbacks that influence regional climate change  
656 and needs for adaptation.

657 **Code and Data Availability**

658 All of the research input data and codes supporting the results reported in this paper are available  
659 in a repository (<https://doi.org/10.5281/zenodo.7927852>, Shrestha et al., 2023).

660 **Author Contribution**

661 The first author conceptualized and designed the research, curated data, ran the analysis and wrote  
662 a draft. The second author (Dr. Christopher A. Williams) provided substantial input in research  
663 conceptualization, research framework, and polishing of the manuscript. Drs. Brendan M. Rogers,  
664 John Rogan, and Dominik Kulakowski offered insight into the manuscript's data analysis  
665 presentation and contributed to the draft manuscript's finalization.

666 **Conflict of Interest**

667 The authors declare that they have no known competing financial interests or personal  
668 relationships that could have appeared to influence the work reported in this paper.

669

670 **References**

671 Abatzoglou, J. T., Williams, A. P.: Impact of anthropogenic climate change on wildfire across  
672 western US forests, *Proceedings of the National Academy of Sciences*, 113(42), 11770–  
673 11775. <http://doi.org/10.1073/pnas.1607171113>, 2016.

674 Abdul Halim, M., Chen, H. Y. H., Thomas, S. C.: Stand age and species composition effects on  
675 surface albedo in a mixedwood boreal forest, *Biogeosciences* 16, 4357–4375.  
676 <https://doi.org/10.5194/bg-16-4357-2019>, 2019.

677 Allen, C.D., Breshears, D.D., McDowell, N.G.: On underestimation of global vulnerability to tree  
678 mortality and forest die-off from hotter drought in the Anthropocene, *Ecosphere* 6: 1–55.  
679 <https://doi.org/10.1890/ES15-00203.1>, 2015.

680 Amiro, B.D., Barr, A.G., Barr, J.G., Black, T.A., Bracho, R., Brown, M., Chen, J., Clark, K.L.,  
681 Davis, K.J., Desai, A.R., Dore, S., Engel, V., Fuentes, J.D., Goldstein, A.H., Goulden,  
682 M.L., Kolb, T.E., Lavigne, M.B., Law, B.E., Margolis, H.A., Martin, T., McCaughey, J.H.,  
683 Misson, L., Montes-Helu, M., Noormets, A., Randerson, J.T., Starr, G., Xiao, J.:  
684 Ecosystem carbon dioxide fluxes after disturbance in forests of North America, *J. Geophys.  
685 Res. Biogeosciences* 115. <https://doi.org/10.1029/2010JG001390>, 2010.

686 Amiro, B.D., Chen, J.M., Liu, J.: Net primary productivity following forest fire for Canadian  
687 ecoregions, *Can. J. For. Res.* 30, 939–947. <https://doi.org/10.1139/cjfr-30-6-939>, 2000.

688 Amiro, B.D., Orchansky, A.L., Barr, A.G., Black, T.A., Chambers, S.D., Chapin, F.S., Goulden,  
689 M.L., Litvak, M., Liu, H.P., McCaughey, J.H., McMillan, A., Randerson, J.T.: The effect  
690 of post-fire stand age on the boreal forest energy balance, *Agric. For. Meteorol.* 140, 41–

691 50. <https://doi.org/10.1016/j.agrformet.2006.02.014>, 2006.

692 Bartlein, P.J., Hostetler, S.W.: Modeling paleoclimates, Dev. Quat. Sci. 1, 565–584,

693 [https://doi.org/10.1016/S1571-0866\(03\)01027-3](https://doi.org/10.1016/S1571-0866(03)01027-3), 2003.

694 Barton, A.M.: Intense wildfire in southeastern Arizona: Transformation of a Madrean oak-pine

695 forest to oak woodland, For. Ecol. Manage. 165, 205–212, [https://doi.org/10.1016/S0378-1127\(01\)00618-1](https://doi.org/10.1016/S0378-1127(01)00618-1), 2002.

696

697 Beck, P. S. A., Goetz, S. J., Mack, M. C., Alexander, H. D., Jin, Y., Randerson, J. T., and Loranty,

698 M. M.: The impacts and implications of an intensifying fire regime on Alaskan boreal

699 forest composition and albedo, Global Change Biol., 17, 2853–2866, doi:10.1111/j.1365-

700 2486.2011.02412.x., 2011.

701 Besnard, S., Koirala, S., Santoro, M., Weber, U., Nelson, J., Gütter, J., Herault, B., Kassi, J.,

702 N'Guessan, A., Neigh, C., Poulter, B., Zhang, T., and Carvalhais, N.: Mapping global forest

703 age from forest inventories, biomass and climate data, Earth Syst. Sci. Data, 13, 4881–

704 4896, <https://doi.org/10.5194/essd-13-4881-2021>, 2021.

705 Betts, A., Ball, J.: Albedo over the boreal forest. *Journal of Geophysical Research* **102**, 28 901–

706 28 609, doi:10.1029/96JD03876, 1997.

707 Bond-Lamberty, B., Peckham, S.D., Gower, S.T., Ewers, B.E.: Effects of fire on regional

708 evapotranspiration in the central Canadian boreal forest, Glob. Chang. Biol. 15, 1242–

709 1254, <https://doi.org/10.1111/j.1365-2486.2008.01776.x>, 2009.

710 Boschetti, L., Roy, D.P., Justice, C.O., Humber, M.L.: MODIS–Landsat fusion for large area 30

711 m burned area mapping, Remote Sensing of Environment, 161, 27–42, 2015.

712 Breiman, L.: Random forests, Machine Learning 45: 5–32, <https://doi.org/10.1023/A:1010933404324>, 2001.

713

714 Bright, B.C., Hudak, A.T., Kennedy, R.E., Braaten, J.D., Henareh Khalyani, A.: Examining post-  
715 fire vegetation recovery with Landsat time series analysis in three western North American  
716 forest types, Fire Ecol. 15, <https://doi.org/10.1186/s42408-018-0021-9>, 2019.

717 Bright, R. M., Zhao, K., Jackson, R. B., and Cherubini, F.: Quantifying surface albedo and other  
718 direct biogeophysical climate forcings of forestry activities, Global Change Biol., 21,  
719 3246–3266, <https://doi.org/10.1111/gcb.12951>, 2015.

720 Brown, P.M., and Wu, R.: Climate and disturbance forcing of episodic tree recruitment in a  
721 Southwestern ponderosa pine landscape, Ecology 86: 3030–3038, doi: [10.1890/05-0034](https://doi.org/10.1890/05-0034),  
722 2005.

723 Buechling, A., Martin, P.H., Canham, C.D., Shepperd, W.D., Battaglia, M.A., Rafferty, N.:  
724 Climate drivers of seed production in *picea engelmannii* and response to warming  
725 temperatures in the Southern Rocky Mountains, J. Ecol. 104, 1051–1062,  
726 <https://doi.org/10.1111/1365-2745.12572>, 2016.

727 Campagnolo, M. L., Sun, Q., Liu, Y., Schaaf, C., Wang, Z., Román, M. O.: Estimating the effective  
728 spatial resolution of the operational BRDF, albedo, and nadir reflectance products from  
729 MODIS and VIIRS, *Remote Sensing of Environment*, 175, 52–64,  
730 <https://doi.org/10.1016/j.rse.2015.12.033>, 2016.

731 Campbell, J., Donato, D. Azuma, D. Law, B.: Pyrogenic carbon emission from a large wildfire in  
732 Oregon, United States, J. Geophys. Res., 112, G04014, doi:10.1029/2007JG000451, 2007.

733 Cansler, C.A., Mckenzie, D.: Climate, fire size, and biophysical setting control fire severity and  
734 spatial pattern in the northern Cascade Range, USA. *Ecol. Appl.* 24, 1037–1056,  
735 <https://doi.org/10.1890/13-1077.1>, 2014.

736 Casady, G.M., van Leeuwen, W.J.D., Marsh, S.E.: Evaluating Post-wildfire Vegetation  
737 Regeneration as a Response to Multiple Environmental Determinants, *Environ. Model.*  
738 *Assess.* 15, 295–307, <https://doi.org/10.1007/s10666-009-9210-x>, 2010.

739 Chambers, M. E., Fornwalt, P. J., Malone, S. L. and Battaglia, M. A.: Patterns of conifer  
740 regeneration following high severity wildfire in ponderosa pine-dominated forests of the  
741 Colorado Front Range, *Forest Ecology and Management*, 378:57–67, 2016.

742 Chambers, S. D., Beringer, J., Randerson, J. T., Chapin, I. S.: Fire effects on net radiation and  
743 energy partitioning: Contrasting responses of tundra and boreal forest ecosystems, *J.*  
744 *Geophys. Res.* 110, 1–9, <https://doi.org/10.1029/2004JD005299>, 2005.

745 Chambers, S. D., Chapin III, F. S.: Fire effects on surface-atmosphere energy exchange in Alaskan  
746 black spruce ecosystems Fire effects on surface-atmosphere energy exchange in Alaskan  
747 black spruce ecosystems: Implications for feedbacks to regional climate, *J. Geophys. Res.*  
748 107, 8145, <https://doi.org/10.1029/2001JD000530>, 2002.

749 Chappell, C. B., Agee, J. K.: Fire severity and tree seedling establishment in *Abies magnifica*  
750 forests, southern Cascades, Oregon, *Ecological Applications*, 6, 628–640.  
751 <https://doi.org/10.2307/2269397>, 1996.

752 Chen, X., Vogelmann, J. E., Rollins, M., Ohlen, D., Key, C. H., Yang, L., Huang, C., Shi, H.:  
753 Detecting post-fire burn severity and vegetation recovery using multitemporal remote  
754 sensing spectral indices and field-collected composite burn index data in a ponderosa pine

755 forest, Int. J. Remote Sens. 32, 7905–7927,  
756 <https://doi.org/10.1080/01431161.2010.524678>, 2011.

757 Cohen, W.B., Maiersperger, T. K., Turner, D. P., Ritts, W. D., Pflugmacher, D., Kennedy, R. E.,  
758 Kirschbaum, A., Running, S. W., Costa, M., Gower, S. T.: MODIS land cover and LAI  
759 collection 4 product quality across nine sites in the western hemisphere, IEEE Trans.  
760 Geosci. Remote Sens. 44, 1843–1857, <https://doi.org/10.1109/TGRS.2006.876026>, 2006.

761 Crotteau, J. S., Varner III, J. M., and Ritchie, M. W.: Post-fire regeneration across a fire severity  
762 gradient in the southern Cascades, Forest Ecology and Management 287: 103–112,  
763 <https://doi.org/10.1016/j.foreco.2012.09.022>, 2013.

764 Csiszar, I., Schroeder, W., Giglio, L., Ellicott, E., Vadrevu, K.P., Justice, C.O., Wind, B.: Active  
765 fires from the Suomi NPP Visible Infrared Imaging Radiometer Suite: Product status and  
766 first evaluation results, Journal of Geophysical Research: Atmospheres, 119, 803–881,  
767 2014.

768 Dale, V. H., Joyce, L. A., Mcnulty, S., Neilson, R. P., Ayres, M. P., Flannigan, M. D., Hanson, P.  
769 J., Irland, L. C., Ariel, E., Peterson, C. J., Simberloff, D., Swanson, F. J., Stocks, B. J.,  
770 Wotton, B. M., Dale, V. H., Joyce, L. A., Mcnulty, S., Ronald, P., Matthew, P., Simberloff,  
771 D., Swanson, F. J., Stocks, B. J., Wotton, B. M.: Climate Change and Forest Disturbances,  
772 Bioscience, 51(9), 723–734, doi:10.1641/0006-3568(2001)051[0723:CCAFD]2.0.CO;2,  
773 2001.

774 Daly, C., Halbleib, M., Smith, J. I., Gibson, W. P., Doggett, M. K., Taylor, G. H., Curtis, J., and  
775 Pasteris, P. A.: Physiographically-sensitive mapping of temperature and precipitation

776 across the conterminous United States, International Journal of Climatology 28, 2031–  
777 2064, 2008.

778 Davis, K. T., Higuera, P. E., Dobrowski, S. Z., Parks, S. A., Abatzoglou, J. T., Rother, M. T.,  
779 Veblen, T. T.: Fire-catalyzed vegetation shifts in ponderosa pine and Douglas-fir forests of  
780 the western United States, Environ. Res. Lett. 15, <https://doi.org/10.1088/1748-9326/abb9df>, 2020.

782 De Sales, F., Okin, G.S., Xue, Y., Dintwe, K.: On the effects of wildfires on precipitation in  
783 southern Africa, Clim Dyn 52:951–967, <https://doi.org/10.1007/s00382-018-4174-7>, 2018.

784 De Santis, A., Chuvieco, E.: GeoCBI: A modified version of the Composite Burn Index for the  
785 initial assessment of the short-term burn severity from remotely sensed data, Remote  
786 Sensing of Environment, 113, 554–562, 2009.

787 Dennison, P. E., Brewer, S. C., Arnold, J. D., Moritz, M. A.: Large wildfire trends in the western  
788 United States, 1984–2011, Geophysical Research Letters, 41, 2928–2933,  
789 <https://doi.org/10.1002/2014GL059576>, 2014.

790 Dintwe, K., Okin, G.S., Xue, Y.: Fire-induced albedo change and surface radiative forcing in sub-  
791 Saharan Africa savanna ecosystems: Implications for the energy balance, J. Geophys. Res.  
792 122, 6186–6201, <https://doi.org/10.1002/2016JD026318>, 2017.

793 Dore, A. S., Kolb, T. E., Eckert, S. E., Sullivan, B. W., Hungate, B. A., Kaye, J. P., Hart, S. C.,  
794 Koch, G. W., Finkral, A., Applications, S. E., April, N., Dore, S., Kolb, T. E., Eckert, S.  
795 E., Sullivan, W., Hungate, B. A., Kaye, J. P.: Carbon and water fluxes from ponderosa pine  
796 forests disturbed by wildfire and thinning, Ecol. Appl. 20, 663–683, 2010.

797 Downing, W.M., Krawchuk, M.A., Meigs, G.W., Haire, S.L., Coop, J.D., Walker, R.B., Whitman,  
798 E., Chong, G., Miller, C.: Influence of fire refugia spatial pattern on post-fire forest  
799 recovery in Oregon's Blue Mountains, *Landsc. Ecol.* 34, 771–792,  
800 <https://doi.org/10.1007/s10980-019-00802-1>, 2019.

801 Dugan, A. J., Baker, W. L.: Sequentially contingent fires, droughts and pluvials structured a  
802 historical dry forest landscape and suggest future contingencies, *J. Veg. Sci.*, **26**, 697–710,  
803 2015.

804 Dwyer, D. D., Pieper, R. D.: Fire effects on blue gramma-pinyon-juniper rangeland in New  
805 Mexico, *Journal of Range Management*, 20, 359-362, 1967.

806 Eidenshink, J., Schwind, B., Brewer, K., Zhu, Z., Quayle, B., Howard, S., Falls, S., Falls, S.: A  
807 project for monitoring trends in burn severity, *Fire Ecology Special Issue 3*, 3–21, 2007.

808 Epting, J., Verbyla, J.: Landscape-level interactions of prefire vegetation, burn severity, and  
809 postfire vegetation over a 16-year period in interior Alaska, *Canadian Journal of Forest  
810 Research* 35, 1367–1377, <https://doi.org/10.1139/X05-060>, 2005.

811 Erdman, J. A.: Pinyon-juniper succession alter natural fires on residual soils of Mesa Verde,  
812 Colorado, *BYU Science Bulletin in Biology Series*, 11(2), 1970.

813 Ferguson, D. E., Carlson, C. E.: Height-age relationships for regeneration-size trees in the northern  
814 Rocky Mountains, USA, *Research Paper RMRS-RP-82WWW*, USDA Forest Service,  
815 Rocky Mountain Research Station, Fort Collins, Colorado, USA, 2010.

816 Frazier, R. J., Coops, N. C., Wulder, M. A., Hermosilla, T., White, J. C.: Analyzing spatial and  
817 temporal variability in short-term rates of post-fire vegetation return from Landsat time  
818 series, *Remote Sensing of Environment* 205, 32–45, 2018.

819 Gao, F., Schaaf, C.B., Strahler, A.H., Roesch, A., Lucht, W., Dickinson, R.: MODIS bidirectional  
820 reflectance distribution function and albedo Climate Modeling Grid products and the  
821 variability of albedo major global vegetation types, *J. Geophys. Res. D Atmos.* 110, 1–13,  
822 <https://doi.org/10.1029/2004JD005190>, 2005.

823 Gatebe, C. K., Ichoku, C. M., Poudyal, R., Román, M. O., Wilcox, E.: Surface albedo darkening  
824 from wildfires in northern sub-Saharan Africa, *Environ. Res. Lett.*, 9(6), 065003,  
825 doi:10.1088/1748-9326/9/6/065003, 2014.

826 Ghimire, B., Williams, C. A., Collatz, G. J., Vanderhoof, M.: Fire-induced carbon emissions and  
827 regrowth uptake in western U.S. forests: Documenting variation across forest types, fire  
828 severity, and climate regions, *J. Geophys. Res.*, 117, G03036, doi:10.1029/2011JG001935,  
829 2012.

830 Gleason, K.E., McConnell, J.R., Arienzo, M.M., Chellman, N., Calvin, W.M.: Four-fold increase  
831 in solar forcing on snow in western U.S. burned forests since 1999, *Nat. Commun.* 10, 1–  
832 8, <https://doi.org/10.1038/s41467-019-09935-y>, 2019.

833 Gray, A. N., Zald, H. S., Kern, R. A., North, M.: Stand conditions associated with tree regeneration  
834 in Sierran mixed-conifer forests, *Forest Science*, 51, 198–210, 2005.

835 Guz, J., Gill, N.S., Kulakowski, D.: Long-term empirical evidence shows post-disturbance climate  
836 controls post-fire regeneration, *Journal of Ecology*, <https://doi.org/10.1111/1365-2745.13771>, 2021.

838 Haffey, C., Sisk, T. D., Allen, C. D., Thode, A. E., Margolis, E. Q.: Limits to Ponderosa Pine  
839 Regeneration following Large High-Severity Forest Fires in the United States Southwest,  
840 Fire Ecol. 14, 143–163, <https://doi.org/10.4996/fireecology.140114316>, 2018.

841 Haire, S. L., and McGarigal, K.: Effect of landscape patterns of fire severity on regenerating  
842 ponderosa pine forests (*Pinus ponderosa*) in New Mexico and Arizona, USA, Landscape  
843 Ecology, 25, 1055–1069, 2010.

844 Hankin, L. E., Higuera, P. E., Davis, K. T., Dobrowski, S. Z.: Impacts of growing-season climate  
845 on tree growth and post-fire regeneration in ponderosa pine and Douglas-fir forests,  
846 Ecosphere 10, <https://doi.org/10.1002/ecs2.2679>, 2019.

847 Hansen, W. D., Romme, W. H., Ba, A., and Turner, M. G.: Shifting ecological filters mediate  
848 postfire expansion of seedling aspen (*Populus tremuloides*) in Yellowstone, Forest Ecology  
849 and Management, 362, 218–230, 2016.

850 Hartsell, J. A., Copeland, S. M., Munson, S. M., Butterfield, B. J., and Bradford, J. B.: Gaps and  
851 hotspots in the state of knowledge of pinyon-juniper communities, Forest Ecology and  
852 Management 455, 1–23, 2020.

853 Harvey, B. J., Donato, D. C., Turner, M. G.: High and dry: postfire tree seedling establishment in  
854 subalpine forests decreases with post-fire drought and large stand-replacing burn patches,  
855 Global Ecology and Biogeography 25, 655–669. <https://doi.org/10.1111/geb.12443>, 2016.

856 Hicke, J. A., Asner, G. P., Kasischke, E. S., French, N. H. F., Randerson, J. T., Collatz, G. J.,  
857 Stocks, B. J., Tucker, C. J., Los, S. O., Field, C. B.: Postfire response of North American  
858 boreal forest net primary productivity analyzed with satellite observations, Global Change  
859 Biol., 9(8), 1145–1157, doi:10.1046/j.1365-2486.2003.00658.x, 2003.

860 Hislop, S., Haywood, A., Jones, S., Soto-Berelov, M., Skidmore, A., and Nguyen, T. H.: A  
861 satellite data driven approach to monitoring and reporting fire disturbance and recovery  
862 across boreal and temperate forests, *Int. J. Appl. Earth Obs. Geoinf.*, 87, 102034,  
863 <https://doi.org/10.1016/j.jag.2019.102034>, 2020.

864 Howard, J. L.: *Pinus ponderosa* var. *brachyptera*, *P. p.* var. *scopulorum*. Fire Effects Information  
865 System. US Department of Agriculture, Forest Service, Rocky Mountain Research Station,  
866 Fire Sciences Laboratory, Missoula, Montana, USA,  
867 <https://www.fs.fed.us/database/feis/plants/tree/pinpons/all.html>, 2003.

868 Huesca, M., Merino-de-Miguel, S., González-Alonso, F., Martínez, S., Miguel Cuevas, J., Calle,  
869 A.: Using AHS hyper-spectral images to study forest vegetation recovery after a fire,  
870 *International Journal of Remote Sensing*, 34, 4025–4048, 2013.

871 IPCC [Intergovernmental Panel on Climate Change].: Climate change 2007: Synthesis report.  
872 Intergovernmental Panel on Climate Change, 2007.

873 IPCC [Intergovernmental Panel on Climate Change].: Climate change 2013: the physical science  
874 basis. Contribution of Working Group I to the fifth assessment report of the  
875 Intergovernmental Panel on Climate Change, Pages 1-1535 in: T.F. Stocker, D. Qin, G.-K.  
876 Plattner, M. Tignor, S.K. Allen, J. Boschung, A. Nauels, Y. Xia, V. Bex, and P.M. Midgley,  
877 editors. Cambridge University Press, Cambridge, England, United Kingdom, and New  
878 York, New York, USA, 2013.

879 Jameson, D. A.: Effects of burning on galleta-black gramma range invaded by juniper, *Ecology*  
880 43, 760-763, 1962.

881 Jin, Y., Randerson, J. T., Goetz, S. J., Beck, P. S. A., Loranty, M. M., Goulden, M. L.: The

882 influence of burn severity on postfire vegetation recovery and albedo change during early  
883 succession in North American boreal forests, *J. Geophys. Res. Biogeosciences* 117, 1–15,  
884 <https://doi.org/10.1029/2011JG001886>, 2012.

885 Jin, Y., Roy, D. P.: Fire-induced albedo change and its radiative forcing at the surface in northern  
886 Australia, *Geophys. Res. Lett.* 32, 1–4, <https://doi.org/10.1029/2005GL022822>, 2005.

887 Johnstone, J. F., Hollingsworth, T. N., Chapin, F. S., and Mack, M. C.: Changes in fire regime  
888 break the legacy lock on successional trajectories in Alaskan boreal forest, *Global Change  
889 Biol.*, 16, 1281–1295, <https://doi.org/10.1111/j.1365-2486.2009.02051.x>, 2010.

890 Johnstone, J. F., Allen, C. D., Franklin, J. F., Frelich, L. E., Harvey, B. J., Higuera, P. E., Mack,  
891 M. C., Meentemeyer, R. K., Metz, M. R., Perry, G. L., Schoennagel, T., Turner, M. G.:  
892 Changing disturbance regimes, ecological memory, and forest resilience, *Frontiers in  
893 Ecology and the Environment*, 14, 369–378, doi: 10.1002/fee.1311, 2016.

894 Kane, V. R., North, M. P., Lutz, J. A., Churchill, D. J., Roberts, S. L., Smith, D. F., ... Brooks, M.  
895 L.: Assessing fire effects on forest spatial structure using a fusion of Landsat and airborne  
896 LiDAR data in Yosemite National Park, *Remote Sensing of Environment*, 151, 89–101,  
897 2014.

898 Keeley, J. E., Brennan, T., Pfaff, A. H.: Fire severity and ecosystem responses following crown  
899 fires in California shrublands, *Ecol. Appl.* 18, 1530–1546, [https://doi.org/10.1890/07-  
900 0836.1](https://doi.org/10.1890/07-0836.1), 2008.

901 Kemp, K. B., Higuera, P. E., Morgan, P., Abatzoglou, J. T.: Climate will increasingly determine  
902 post-fire tree regeneration success in low-elevation forests, Northern Rockies, USA,  
903 *Ecosphere*, 10, <https://doi.org/10.1002/ecs2.2568>, 2019.

904 Kemp, K.B., Higuera, P.E., Morgan, P.: Fire legacies impact conifer regeneration across  
905 environmental gradients in the US northern Rockies, *Landscape Ecology*, 31, 619–636,  
906 <https://doi.org/10.1007/s10980-015-0268-3>, 2016.

907 Key, C.: Ecological and sampling constraints on defining landscape fire severity, *Fire Ecology* 2,  
908 34–59, doi:10.4996/FIREECOLOGY, 0202034, 2006.

909 Koniak, S.: Succession in pinyon-juniper woodlands following wildfire in the Great Basin, *Great*  
910 *Basin Naturalist*, 45, 556-566, 1985.

911 Kuusinen, N., Tomppo, E., Shuai, Y., Berninger, F.: Effects of forest age on albedo in boreal  
912 forests estimated from MODIS and Landsat albedo retrievals, *Remote Sens. Environ.*, 145,  
913 145–153, <https://doi.org/10.1016/j.rse.2014.02.005>, 2014.

914 Lawrence, P. J., Chase, T. N.: Representing a new MODIS consistent land surface in the  
915 Community Land Model (CLM 3.0), *Journal of Geophysical Research: Biogeosciences*,  
916 112(1), <http://doi.org/10.1029/2006JG000168>, 2007.

917 Lhermitte, S., Verbesselt, J., Verstraeten, W.W., Coppin, P.: A pixel-based regeneration index  
918 using time series similarity and spatial context, *Photogrammetric Engineering and Remote*  
919 *Sensing*, 76, 673–682, 2010.

920 Liaw, A., Wiener, M.: Classification and regression by random forest, *R News*, 2(3), 18–22, 2002.

921 Lippok, D., Beck, S. G., Renison, D., Gallegos, S. C., Saavedra, F. V., Hensen, I., Schleuning, M.:  
922 Forest recovery of areas deforested by fire increases with elevation in the tropical Andes,  
923 *For. Ecol. Manage.* 295, 69–76, <https://doi.org/10.1016/j.foreco.2013.01.011>, 2013.

924 Littell J. S., Mckenzie, D., Wan, H. Y., Cushman, S. A.: Climate change and future wildfire in the

925 Western United States: an ecological approach to nonstationarity, *Earth's Future*, **6**, 1097–  
926 111, 2018.

927 Littell, J. S., Mckenzie, D., Peterson, D. L., Westerling, A. L.: Climate and wildfire area burned in  
928 western U.S. ecoregions, 1916–2003, *Ecological Applications*, **19**(4), 1003–1021, 2009.

929 Littlefield, C. E., Dobrowskia, S. Z., Abatzoglou, J. T., Parks, S. A., and Davise, K. T.: A  
930 climatic dipole drives short- and long-term patterns of postfire forest recovery in the  
931 western United States, *Proc. Natl. Acad. Sci. U. S. A.*, **117**, 29730–29737,  
932 <https://doi.org/10.1073/pnas.2007434117>, 2020.

933 Liu, H., Randerson, J. T., Lindfors, J., Iii, F. S. C.: Changes in the surface energy budget after fire  
934 in boreal ecosystems of interior Alaska: An annual perspective, *Journal of Geophysical  
935 Research Atmospheres*, **110**, 1–12, <https://doi.org/10.1029/2004JD005158>, 2005.

936 Liu, Z.: Effects of climate and fire on short-term vegetation recovery in the boreal larch forests of  
937 northeastern China, *Scientific Reports* **6**, 37572, <https://doi.org/10.1038/srep37572>, 2016.

938 Lydersen, J., North, M.: Topographic variation in structure of mixed-conifer forests under an  
939 active-fire regime, *Ecosystems*, **15**, 1134–1146, 2012.

940 Lyons, E. A., Jin, Y., Randerson, J. T.: Changes in surface albedo after fire in boreal forest  
941 ecosystems of interior Alaska assessed using MODIS satellite observations, *J. Geophys.  
942 Res. Biogeosciences* **113**, 1–15, <https://doi.org/10.1029/2007JG000606>, 2008.

943 Ma, Q., Bales, R. C., Rungee, J., Conklin, M. H., Collins, B. M., Goulden, M. L.: Wildfire controls  
944 on evapotranspiration in California's Sierra Nevada, *J. Hydrol.* **590**, 125364,  
945 <https://doi.org/10.1016/j.jhydrol.2020.125364>, 2020.

946 Maina, F. Z., Siirila-Woodburn, E. R.: Watersheds dynamics following wildfires: Nonlinear  
947 feedbacks and implications on hydrologic responses, *Hydrol. Process.* 34, 33–50,  
948 <https://doi.org/10.1002/hyp.13568>, 2019.

949 Martí 'n-Alcon, S., Coll, L.: Unraveling the relative importance of factors driving post-fire  
950 regeneration trajectories in non-serotinous *Pinus nigra* forests, *Forest Ecology and*  
951 *Management*, 361, 13–22, 2016.

952 Martin, D. P.: Partial dependence plots. <http://dpmartin42.github.io/posts/r/partial-dependence>,  
953 2014.

954 McDowell, N. G., Williams, A. P., Xu, C., Pockman, W. T., Dickman, L. T., Sevanto, S., Pangle,  
955 R., Limousin, J. M., Plaut, J., Mackay, D. S., Ogee, J., Domec, J. C., Allen, C. D., Fisher,  
956 R. A., Jiang, X., Muss, J. D., Breshears, D. D., Rauscher, S. A., Koven, C.: Multi-scale  
957 predictions of massive conifer mortality due to chronic temperature rise, *Nature Climate*  
958 *Change*, 6, 295–300, doi: 10.1038/nclimate2873, 2015.

959 McMichael, C. E., Hope, A. S., Roberts, D. A., Anaya, M. R.: Post-fire recovery of leaf area index  
960 in California chaparral: A remote sensing-chronosequence approach, *Int. J. Remote Sens.*  
961 25, 4743–4760, <https://doi.org/10.1080/01431160410001726067>, 2004.

962 Meigs, G. W., Donato, D. C., Campbell, J. L., Martin, J. G., Law, B. E.: Forest fire impacts on  
963 carbon uptake, storage, and emission: The role of burn severity in the Eastern Cascades,  
964 Oregon, *Ecosystems* (N. Y.), 12(8), 1246–1267, doi:10.1007/s10021-009-9285-x, 2009.

965 Meng, R., Dennison, P. E., D'Antonio, C. M., Moritz, M. A.: Remote sensing analysis of  
966 vegetation recovery following short-interval fires in Southern California Shrublands, *PLoS*  
967 One 9, 14–17, <https://doi.org/10.1371/journal.pone.0110637>, 2014.

968 Meng, R., Dennison, P. E., Huang, C., Moritz, M. A., D'Antonio, C.: Effects of fire severity and  
969 post-fire climate on short-term vegetation recovery of mixed-conifer and red fir forests in  
970 the Sierra Nevada Mountains of California, *Remote Sens. Environ.*, 171, 311–325,  
971 <https://doi.org/10.1016/j.rse.2015.10.024>, 2015.

972 Meng, R., Wu, J., Zhao, F., Cook, B.D., Hanavan, R.P., Serbin, S.P.: Measuring short-term post-  
973 fire forest recovery across a burn severity gradient in a mixed pine-oak forest using multi-  
974 sensor remote sensing techniques, *Remote Sensing of Environment*, 210, 282–296,  
975 <https://doi.org/10.1016/j.rse.2018.03.019>, 2018.

976 Micheletty, P.D., Kinoshita, A.M., Hogue, T.S.: Application of MODIS snow cover products:  
977 Wildfire impacts on snow and melt in the Sierra Nevada, *Hydrol. Earth Syst. Sci.* 18, 4601–  
978 4615, <https://doi.org/10.5194/hess-18-4601-2014>, 2014.

979 Moghaddas, J. J., York, R. A., Stephens, S. L.: Initial response of conifer and California black oak  
980 seedlings following fuel reduction activities in a Sierra Nevada mixed conifer forest, *Forest  
981 Ecology and Management* 255, 3141–3150, 2008.

982 Montes-Helu, M.C., Kolb, T., Dore, S., Sullivan, B., Hart, S.C., Koch, G., Hungate, B.A.:  
983 Persistent effects of fire-induced vegetation change on energy partitioning and  
984 evapotranspiration in ponderosa pine forests, *Agric. For. Meteorol.* 149, 491–500,  
985 <https://doi.org/10.1016/j.agrformet.2008.09.011>, 2009.

986 Morresi, D., Vitali, A., Urbinati, C., Garbarino, M.: Forest spectral recovery and regeneration  
987 dynamics in stand replacing wildfires of central Apennines derived from Landsat time  
988 series, *Remote Sensing* 11, 308, 1–18, 2019.

989 Myhre, G., Kvalevåg, M. M., Schaaf, C. B.: Radiative forcing due to anthropogenic vegetation

990 change based on MODIS surface albedo data, *Geophys. Res. Lett.*, 32,  
991 doi:10.1029/2005GL024004, 2005.

992 Myneni, R. B., Hoffman, S., Knyazikhin, Y., Privette, J. L., Glassy, J., Tian, Y., Wang, Y., Song,  
993 X., Zhang, Y., Smith, G. R., Lotsch, A., Friedl, M., Morisette, J. T., Votava, P., Nemani,  
994 R. R., Running, S. W.: Global products of vegetation leaf area and fraction absorbed PAR  
995 from year one of MODIS data, *Remote Sens. Environ.*, 83, 214–231,  
996 [https://doi.org/10.1016/S0034-4257\(02\)00074-3](https://doi.org/10.1016/S0034-4257(02)00074-3), 2002.

997 O'Halloran, T.L., Acker, S.A., Joerger, V.M., Kertis, J., Law, B.E.: Postfire influences of snag  
998 attrition on albedo and radiative forcing, *Geophys. Res. Lett.* 41, 9135–9142,  
999 <https://doi.org/10.1002/2014GL062024>, 2014.

1000 Parks, S.A., Dillon, G.K., Miller, C.: A new metric for quantifying burn severity: the Relativized  
1001 Burn Ratio, *Remote Sensing*, 6, 1827–1844, 2014.

1002 Pinty, B., Verstraete, M. M., Gobron, N., Govaerts, Y., Roveda, F.: Do human-induced fires affect  
1003 the Earth surface reflectance at continental scales? *EOS Trans. Am. Geophys. Union* 81  
1004 381–9, 2000.

1005 Polychronaki, A., Gitas, I. Z., Minchella, A.: Monitoring post-fire vegetation recovery in the  
1006 Mediterranean using SPOT and ERS imagery, *International Journal of Wildland Fire*, 23,  
1007 631–642, 2013.

1008 Potter, S., Solvik, K., Erb, A., Goetz, S. J., Johnstone, J. F., Mack, M. C., Randerson, J. T., Roman,  
1009 M. O., Schaaf, C. L., Turetsky, M. R., Veraverbeke, S., Walker, X. J., Wang, Z., Massey,  
1010 R., and Rogers, B. M.: Climate change decreases the cooling effect from postfire albedo in

1011 boreal North America, *Glob. Change Biol.*, 26, 1592–1607,

1012 <https://doi.org/10.1111/gcb.14888>, 2020.

1013 Randerson, J. T., Liu, H., Flanner, M. G., Chambers, S. D., Jin, Y., Hess, P. G., Pfister, G., Mack,  
1014 M. C., Treseder, K. K., Welp, L. R., Chapin, F. S., Harden, J. W., Goulden, M. L., Neff, J.  
1015 C., Schuur, E. A. G., Zender, C. S.: The impact of Boreal forest fire on climate warming,  
1016 *Science*, 314, 1130, <https://doi.org/10.1126/science.1132075>, 2006.

1017 Roche, J. W., Goulden, M. L., Bales, R. C.: Estimating evapotranspiration change due to forest  
1018 treatment and fire at the basin scale in the Sierra Nevada, California, *Ecohydrology*, 11,  
1019 <https://doi.org/10.1002/eco.1978>, 2018.

1020 Rodman, K. C., Veblen, T. T., Chapman, T. B., Rother, M. T., Wion, A. P., Redmond, M. D.:  
1021 Limitations to recovery following wildfire in dry forests of southern Colorado and northern  
1022 New Mexico, USA, *Ecological Applications* 30, e02001, 2020.

1023 Rodrigo, A., Retana, J., Picó, F. X.: Direct regeneration is not the only response of Mediterranean  
1024 forests to large fires, *Ecology*, 85, 716–729, 2004.

1025 Knox, K. J. E., Clarke, P. J.: Fire severity, feedback effects and resilience to alternative community  
1026 states in forest assemblages, *Forest Ecology and Management*, 265, 47–54, 2012.

1027 Rogers, B. M., Neilson, R. P., Drapek, R., Lenihan, J. M., Wells, J. R., Bachelet, D., Law, B. E.:  
1028 Impacts of climate change on fire regimes and carbon stocks of the U.S. Pacific Northwest,  
1029 *J. Geophys. Res. Biogeosciences* 116, 1–13, <https://doi.org/10.1029/2011JG001695>, 2011.

1030 Rogers, B. M., Randerson, J. T., Bonan, G. B.: High-latitude cooling associated with landscape  
1031 changes from North American boreal forest fires, *Biogeosciences*, 10, 699–718,

1032 <https://doi.org/10.5194/bg-10-699-2013>, 2013.

1033 Rogers, B. M., Soja, A. J., Goulden, M. L., Randerson, J. T.: Influence of tree species on  
1034 continental differences in boreal fires and climate feedbacks, *Nat. Geosci.* 8, 228–234.

1035 <https://doi.org/10.1038/geo2352>, 2015.

1036 Rother, M. T., Veblen, T. T.: Limited conifer regeneration following wildfires in dry ponderosa  
1037 pine forests of the Colorado Front Range, *Ecosphere* 7, <https://doi.org/10.1002/ecs2.1594>,  
1038 2016.

1039 Rother, M. T., Veblen, T. T.: Climate drives episodic conifer establishment after fire in dry  
1040 ponderosa pine forests of the Colorado Front Range, USA, *Forests*, 8, 1–14,  
1041 <https://doi.org/10.3390/f8050159>, 2017.

1042 Roy, D.P., Boschetti, L., Trigg, S.N.: Remote sensing of fire severity: assessing the performance  
1043 of the normalized burn ratio, *IEEE Geoscience and Remote Sensing Letters*, 3, 112–116,  
1044 2006.

1045 Ruefenacht, B., Finco, M., Czaplewski, R., Helmer, E., Blackard, J., Holden, G., Lister, A.,  
1046 Salajanu, D., Weyermann, D., Winterberger, K.: Conterminous US and Alaska forest type  
1047 mapping using forest inventory and analysis data, *Photogramm. Eng. Remote Sensing* 74,  
1048 1379–1388, 2008.

1049 Russell, R. E., Saab, V. A., Dudley, J. G., Rotella, J. J.: Snag longevity in relation to wildfire and  
1050 postfire salvage logging, *Forest Ecology and Management*, 232, 179–187, 2006.

1051 Salomonson, V. V., Appel, I.: Estimating fractional snow cover from MODIS using the normalized  
1052 difference snow index, *Remote Sensing of Environment*, 89 (3), 351–360,  
1053 <https://doi.org/10.1016/j.rse.2003.10.016>, 2004.

1054 Savage, M., Brown, P. M. Feddema, J.: The role of climate in a pine forest regeneration pulse in  
1055 the southwestern United States, *Ecoscience*, 3, 310–318, 1996.

1056 Schaaf, C. B., Gao, F., Strahler, A. H., Lucht, W., Li, X., Tsang, T., Strugnell, N. C., Zhang, X.,  
1057 Jin, Y., Muller, J., Lewis, P., Barnsley, M., Hobson, P., Disney, M., Roberts, G.,  
1058 Dunderdale, M., Doll, C., Robert, P., Hu, B., Liang, S., Privette, J. L., Roy, D.: First  
1059 operational BRDF, albedo nadir reflectance products from MODIS, *Remote Sens. Environ.*  
1060 83, 135–148, 2002.

1061 Scholze, M., Knorr, W., Arnell, N. W., Prentice, I. C.: A climate-change risk analysis for world  
1062 ecosystems, *Proceedings of the National Academy of Sciences of the United States of  
1063 America*, 103(35), 13116–13120, 2006.

1064 Seastedt, T. R., Hobbs, R. J., Suding, K. N.: Management of novel ecosystems: Are novel  
1065 approaches required? *Frontiers in Ecology and the Environment*, 6, 547–553, 2008.

1066 Shrestha, S., Williams, C.A., Rogan, J., Kulakowski, D., Rogers, B.: Forest types show divergent  
1067 biophysical responses after fire: challenges to ecological modeling , Zenodo [code, data  
1068 set], <https://doi.org/10.5281/zenodo.7927852>, 2023.

1069 Shrestha, S., Williams, C.A., Rogers, B.M., Rogan, J., Kulakowski, D.: Wildfire controls on land  
1070 surface properties in mixed conifer and ponderosa pine forests of Sierra Nevada and  
1071 Klamath mountains, Western US, *Agric. For. Meteorol.* 320, 108939,  
1072 <https://doi.org/10.1016/j.agrformet.2022.108939>, 2022.

1073 Shrestha, S., Williams, C.A., Rogers, B.M., Rogan, J., Kulakowski, D.: Forest Types Show  
1074 Divergent Biophysical Responses After Fire: Challenges to Ecological Modeling [Data  
1075 set], Zenodo, <https://doi.org/10.5281/zenodo.7927852>, 2023.

1076 Stevens-Rumann, C. S., Kemp, K. B., Higuera, P. E., Harvey, B. J., Rother, M. T., Donato, D. C.,  
1077 Morgan, P., Veblen, T. T.: Evidence for declining forest resilience to wildfires under  
1078 climate change, *Ecol. Lett.* 21, 243–252, <https://doi.org/10.1111/ele.12889>, 2018.

1079 Stevens-rumann, C. S., Morgan, P.: Tree regeneration following wildfires in the western US : a  
1080 review 1, 1–17, 2019.

1081 Stoddard, M. T., Huffman, D. W., Fulé, P. Z., Crouse, J. E., Meador, A. J. S.: Forest structure and  
1082 regeneration responses 15 years after wildfire in a ponderosa pine and mixed-conifer  
1083 ecotone, Arizona, USA, *Fire Ecol.* 14, 1–12, <https://doi.org/10.1186/s42408-018-0011-y>,  
1084 2018.

1085 Strobl, C., Boulesteix, A.-L., Zeileis, A., Hothorn, T.: Bias in random forest variable importance  
1086 measures: Illustrations, sources and a solution, *BMC Bioinformatics*, 8, 25,  
1087 <https://doi.org/10.1186/1471-2105-8-25>, 2007.

1088 Thompson, C., Beringer, J., Chapin, F.S., McGuire, A.D.: Structural complexity and land-surface  
1089 energy exchange along a gradient from arctic tundra to boreal forest, *J. Veg. Sci.* 15, 397–  
1090 406, <https://doi.org/10.1111/j.1654-1103.2004.tb02277.x>, 2004.

1091 Thompson, R. S., Shafer, S. L., Strickland, L. E., Van de Water, P. K., Anderson, K. H.: Quaternary  
1092 vegetation and climate change in the western United States: Developments, perspectives,  
1093 and prospects, *Dev. Quat. Sci.* 1, 403–426, [https://doi.org/10.1016/S1571-0866\(03\)01018-2](https://doi.org/10.1016/S1571-0866(03)01018-2), 2003.

1095 Tsuyuzaki, S., Kushida, K., Kodama, Y.: Recovery of surface albedo and plant cover after wildfire  
1096 in a *Picea mariana* forest in interior Alaska, *Climatic Change* 93, 517–525,  
1097 doi:10.1007/S10584-008-9505-Y, 2009.

1098 Urza, A. K., Weisberg, P. J., Chambers, J. C., Dhaemers, J. M., Board, D.: Post-fire vegetation  
1099 response at the woodland–shrubland interface is mediated by the pre-fire community,  
1100 *Ecosphere*, 8, <https://doi.org/10.1002/ecs2.1851>, 2017.

1101 U.S. Geological Survey.: 3D Elevation Program 30-Meter Resolution Digital Elevation Model,  
1102 2019. Assessed December 30, 2019 at <https://www.usgs.gov/the-national-map-data-delivery>

1104 Van Mantgem, P. J., Stephenson, N. L., Keeley, J. E.: Forest reproduction along a climatic gradient  
1105 in the Sierra Nevada, California, For. Ecol. Manage., 225, 391–399,  
1106 <https://doi.org/10.1016/j.foreco.2006.01.015>, 2006.

1107 Vanderhoof, M. K., Hawbaker, T. J., Ku, A., Merriam, K., Berryman, E., Cattau, M.: Tracking  
1108 rates of postfire conifer regeneration vs. deciduous vegetation recovery across the western  
1109 United States, *Ecol. Appl.* 31, <https://doi.org/10.1002/eap.2237>, 2020.

1110 Veraverbeke, S., Gitas, I., Katagis, T., Polychronaki, A., Somers, B., Goossens, R.: Assessing post-  
1111 fire vegetation recovery using red-near infrared vegetation indices: Accounting for  
1112 background and vegetation variability, *ISPRS J. Photogramm. Remote Sens.* 68, 28–39,  
1113 <https://doi.org/10.1016/j.isprsjprs.2011.12.007>, 2012, a.

1114 Veraverbeke, S., Lhermitte, S., Verstraeten, W. W., Goossens, R.: The temporal dimension of  
1115 differenced Normalized Burn Ratio (dNBR) fire/burn severity studies: The case of the large  
1116 2007 Peloponnese wildfires in Greece, *Remote Sens. Environ.* 114, 2548–2563,

1117 <https://doi.org/10.1016/j.rse.2010.05.029>, 2010.

1118 Veraverbeke, S., Verstraeten, W. W., Lhermitte, S., Van De Kerchove, R., Goossens, R.:  
1119 Assessment of post-fire changes in land surface temperature and surface albedo, and their  
1120 relation with fire burn severity using multitemporal MODIS imagery, *Int. J. Wildl. Fire* 21,  
1121 243–256, <https://doi.org/10.1071/WF10075>, 2012, b.

1122 Wangler, M.J., Minnich, R.A.: Fire and Succession in Pinyon-Juniper Woodlands of the San  
1123 Bernardino Mountains, California. Author(s): Michael J . Wangler and Richard A .  
1124 Minnich. Published by : California Botanical Society Stable URL :  
1125 <http://www.jstor.org/stable/41425166>. References 43, 493–514, 1996.

1126 Welch, K. R., Safford, H. D., Young, T. P.: Predicting conifer establishment post wildfire in mixed  
1127 conifer forests of the North American Mediterranean-climate zone, *Ecosphere*, 7,  
1128 <https://doi.org/10.1002/ecs2.1609>, 2016.

1129 Westerling, A. L., Hidalgo, H. G., Cayan, D. R., Swetnam, T. W.: Warming and earlier spring  
1130 increase Western U.S. forest wildfire activity, *Science*, 313(5789), 940–943,  
1131 <http://doi.org/10.1126/science.1128834>, 2006.

1132 Williams, A. P., Abatzoglou, J. T.: Recent Advances and Remaining Uncertainties in Resolving  
1133 Past and Future Climate Effects on Global Fire Activity, *Current Climate Change Reports*,  
1134 2(1), 1–14, <http://doi.org/10.1007/s40641-016-0031-0>, 2016.

1135 Williams, A. P., Seager, R., Berkelhammer, M., Macalady, A. K., Crimmins, M. A., Swetnam, T.  
1136 W., Trugman, A. T., Buenning, N., Hryniw, N., McDowell, N. G., Noone, D., Mora, C. I.,  
1137 Rahn T.: Causes and implications of extreme atmospheric moisture demand during the  
1138 record-breaking 2011 wildfire season in the southwestern United States, *Journal of Applied*

1139 Williams, C. A., Collatz, G. J., Masek, J., Goward, S. N.: Carbon consequences of forest  
1140 disturbance and recovery across the conterminous United States, *Global Biogeochem.*  
1141 *Cycles*, 26(1), GB1005, doi:10.1029/2010GB003947, 2012.

1142 Williams, C.A., Gu, H., Jiao, T.: Climate impacts of U.S. forest loss span net warming to net  
1143 cooling, *Sci. Adv.* 7, 1–7, <https://doi.org/10.1126/sciadv.aax8859>, 2021.

1144 Williams, C.A., Vanderhoof, M.K., Khomik, M., Ghimire, B.: Post-clearcut dynamics of carbon,  
1145 water and energy exchanges in a midlatitude temperate, deciduous broadleaf forest  
1146 environment, *Glob. Chang. Biol.* 20, 992–1007, <https://doi.org/10.1111/gcb.12388>, 2014.

1147 Williams, M., Richardson, A.D., Reichstein, M., Stoy, P.C., Peylin, P., Verbeeck, H., Carvalhais,  
1148 N., Jung, M., Hollinger, D.Y., Kattge, J., Leuning, R., Luo, Y., Tomelleri, E., Trudinger,  
1149 C.M., Wang, Y. P.: Improving land surface models with FLUXNET data, *Biogeosciences*  
1150 6, 1341–1359, 2009.

1151 Wittenberg, L., Malkinson, D., Beeri, O., Halutzy, A., Tesler, N.: Spatial and temporal patterns of  
1152 vegetation recovery following sequences of forest fires in a Mediterranean landscape, Mt.  
1153 Carmel Israel, *Catena* 71, 76–83, <https://doi.org/10.1016/j.catena.2006.10.007>, 2007.

1154 Yang, J., Pan, S. Dangal, S. Zhang, B. Wang, S. Tian. H.: Continental-scale quantification of post-  
1155 fire vegetation greenness recovery in temperate and boreal North America, *Remote Sensing*  
1156 *of Environment* 199, 277–290. <https://doi.org/10.1016/j.rse.2017.07.022>, 2017.

1158 Zhao, F. R., Meng, R., Huang, C., Zhao, M., Zhao, F. A., Gong, P., Yu, L., and Zhu, Z.: Long-  
1159 term post-disturbance forest recovery in the Greater Yellowstone ecosystem analyzed  
1160 using Landsat time series stack, *Remote Sensing* 8, 1–22, 2016.